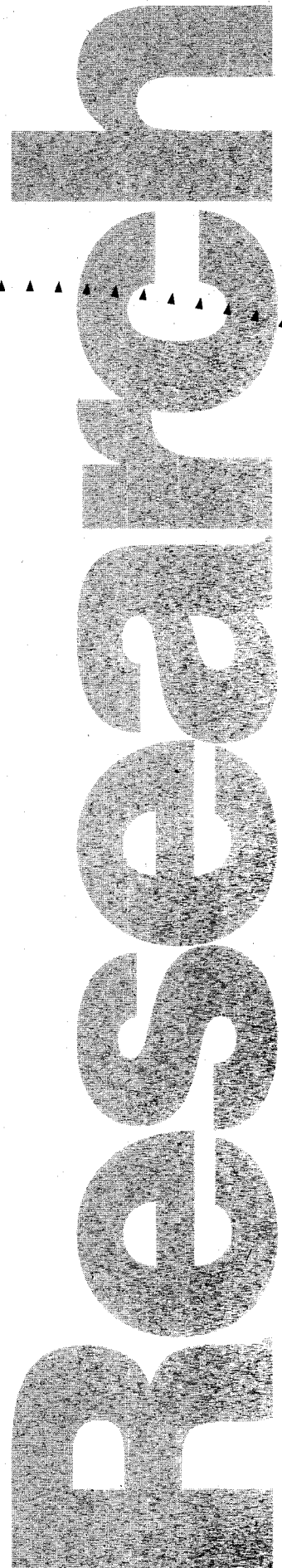


# Analysis of a Differential Global Positioning System as a Sensor for Vehicle Guidance





## Technical Report Documentation Page

1. Report No. <b>MN/RC - 97/17</b>	2.	3. Recipient's Accession No.	
4. Title and Subtitle <b>ANALYSIS OF A DIFFERENTIAL GLOBAL POSITIONING SYSTEM AS A SENSOR FOR VEHICLE GUIDANCE</b>		5. Report Date <b>September 1996</b>	
		6.	
7. Author(s) <b>Robert Bodor, Lee Alexander, Chen-fu Liao, Sundeep Bajikar, Vassilios Morellas, Max Donath</b>		8. Performing Organization Report No.	
9. Performing Organization Name and Address <b>University of Minnesota          Department of Mechanical Engineering          125 MechE Building          111 Church St., S.E.          Minneapolis, MN 55455</b>		10. Project/Task/Work Unit No.	
		11. Contract (C) or Grant (G) No. <b>(C) 73168 TOC # 174</b>	
12. Sponsoring Organization Name and Address <b>Minnesota Department of Transportation          395 John Ireland Boulevard Mail Stop 330          St. Paul, Minnesota 55155</b>		13. Type of Report and Period Covered <b>Final Report 1996</b>	
		14. Sponsoring Agency Code	
15. Supplementary Notes			
16. Abstract (Limit: 200 words) <p>An ongoing research project examines guidance systems, which can take over control of a vehicle if the driver becomes incapacitated. Part of this project includes an evaluation of a Differential Global Positioning System (DGPS) for vehicle-based lane sensing.</p> <p>This report documents the results of tests of the 5 Hz NovAtel RT20 DGPS receiver. A series of 32 static tests found the overall mean and standard deviation for the offset errors within specifications. In a series of dynamic tests, in which the vehicle was driven around the track at speeds of 20-35 miles per hour, after removing the effect of the GPS receiver's latency, the DGPS determined position exhibited a mean offset error of -17.3 cm (-6.82 in) and a mean standard deviation of 25.5 cm (10.1 in) in the direction of vehicle motion. In the direction perpendicular to vehicle motion, the mean offset was 4.57 cm (1.8 in) with a mean standard deviation of 39.6 cm (15.6 in). With no overhead obstructions in these tests, continuous satellite lock was possible. Tests at higher speeds based on a more accurate methodology are planned for the future.</p>			
17. Document Analysis/Descriptors <b>differential global positioning system (DGPS)          vehicle guidance</b>		18. Availability Statement <b>No restrictions. Document available from:          National Technical Information Services,          Springfield, Virginia 22161</b>	
19. Security Class (this report) <b>Unclassified</b>	20. Security Class (this page) <b>Unclassified</b>	21. No. of Pages <b>80</b>	22. Price



# **ANALYSIS OF A DIFFERENTIAL GLOBAL POSITIONING SYSTEM AS A SENSOR FOR VEHICLE GUIDANCE**

## **Final Report**

Prepared by:

Robert Bodor

Lee Alexander

Chen-fu Liao

Sundeep Bajikar

Vassilios Morellas

Max Donath

Department of Mechanical Engineering,  
the Center for Advanced Manufacturing, Design and Control (CAMDAC)

The University of Minnesota

111 Church Street SE  
Minneapolis MN 55455

**September 1996**

Published by

Minnesota Department of Transportation  
Office of Research Administration  
200 Ford Building Mail Stop 330  
117 University Avenue  
St. Paul, MN 55155

This report represents the results of research conducted by the authors and does not necessarily reflect the official views or policies of the Minnesota Department of Transportation. This report does not contain a standard or specified technique.



## Acknowledgments

We would like to thank Ted Morris for his technical assistance with the image processing and Craig Shankwitz for his input at the initial stages of this project.

Thanks are also due to the Minnesota Department of Transportation (Mn/DOT) personnel including Dave Gorg and the Surveying and Mapping Section and Dixon Hoyle of the U.S. Geodetic Survey for providing us with valuable background information and the surveyed data used for the study conducted here. We would especially like to thank Jack Herndon and the others at Mn/ROAD for their flexibility and assistance with the experiments.

This project was partially supported by Mn/DOT, and the Center for Advanced Manufacturing, Design and Control and the Center for Transportation Studies, both at the University of Minnesota, and the Federal Highway Administration of the U.S. Department of Transportation.

We would like to thank Navistar for their assistance with the acquisition of the truck, MTS Systems, Inc. for their assistance with various subsystem design issues, and Andrew and NovAtel for technical assistance regarding their sensors.





## TABLE OF CONTENTS

	Page
CHAPTER 1	INTRODUCTION ..... 1
CHAPTER 2	EVALUATION OF STATIC PERFORMANCE ..... 7
	Description of Experiment..... 7
	Results ..... 9
	Absolute Position Accuracy ..... 9
	Comparison of Static DGPS Accuracy During a Single Test Run.....10
	Static DGPS Accuracy at Individual Survey Nails .....13
	Comparison of Static DGPS Accuracy at the Same Survey Nail .....18
	Absolute Accuracy of Static DGPS .....25
	13 Day Continuous Log .....26
	Relative Accuracy of Static DGPS .....30
	Long Distance Measurements.....30
	Short Distance Measurements.....32
	Effect of Blocking Antenna .....34
CHAPTER 3	EVALUATION OF DYNAMIC PERFORMANCE .....39
	Description of Experiment.....39
	Results.....45
	Error in the Direction of Motion .....50
	Error Perpendicular to the Direction of Motion .....52
	DGPS Error Covariance.....53
	Error Due to Velocity .....54
	Dynamic DGPS Repeatability.....56
CHAPTER 4	CONCLUSIONS.....59
REFERENCES	.....61
APPENDICES	



## List of Tables

Table 2.1	Static DGPS Accuracy During a Single Test Run .....	11
Table 2.2	Static DGPS Accuracy at the Same Survey Nail on the Same Day .....	18
Table 2.3	Static DGPS Accuracy at the Same Survey Nail on Different Days .....	21
Table 2.4	Ensemble Statistics .....	24
Table 2.5	Overall Static DGPS Statistics .....	25
Table 3.1	DGPS Error in the Direction of Motion.....	50
Table 3.2	DGPS Error Perpendicular to the Direction of Motion.....	52
Table 3.3	Dynamic DGPS Covariance.....	53

## List of Figures

Figure 1.1	NovAtel RT20 DGPS accuracy specifications.....	4
Figure 1.2	Mn/ROAD facility (Wright County, MN) .....	5
Figure 1.3	Aerial photograph of Mn/ROAD track .....	6
Figure 1.4	Research building at Mn/ROAD site .....	6
Figure 2.1	Static DGPS accuracy experimental configuration .....	8
Figure 2.2	Pictorial representation of statistical terminology .....	10
Figure 2.3	Static DGPS X offset from true at four survey nails .....	12
Figure 2.4	Static DGPS Y offset from true at four survey nails .....	12
Figure 2.5	Survey nail 63 static DGPS offset from true .....	14
Figure 2.6	Survey nail 63 static DGPS running 25pt standard deviation .....	14
Figure 2.7	Survey nail 90 static DGPS offset from true .....	15
Figure 2.8	Survey nail 90 static DGPS running 25pt standard deviation .....	15
Figure 2.9	Survey nail 101 static DGPS offset from true .....	16

Figure 2.10	Survey nail 101 static DGPS running 25pt standard deviation .....	16
Figure 2.11	Survey nail 175 static DGPS offset from true .....	17
Figure 2.12	Survey nail 175 static DGPS running 25pt standard deviation .....	17
Figure 2.13	Survey nail 63 static DGPS offset from true, run 1 .....	19
Figure 2.14	Survey nail 63 static DGPS offset from true, run 2 .....	19
Figure 2.15	Survey nail 90 static DGPS offset from true, run 1 .....	20
Figure 2.16	Survey nail 90 static DGPS offset from true, run 2 .....	20
Figure 2.17	Survey nail 101 static DGPS offset from true, run 1 .....	22
Figure 2.18	Survey nail 101 static DGPS offset from true, run 3 .....	22
Figure 2.19	Survey nail 219 static DGPS offset from true, run 1 .....	23
Figure 2.20	Survey nail 219 static DGPS offset from true, run 1 .....	23
Figure 2.21	13 day continuous static DGPS log position offset from true.....	27
Figure 2.22	Close-up of X offset during 13 day continuous DGPS log .....	28
Figure 2.23	Close-up of Y offset during 13 day continuous DGPS log .....	28
Figure 2.24	Variation in X over three successive periods of oscillation: worst .....	29
Figure 2.25	Variation in X over three successive periods of oscillation: best .....	29
Figure 2.26	Static DGPS long distance measurements .....	31
Figure 2.27	Static DGPS error in long distance measurements .....	31
Figure 2.28	Static DGPS short distance measurements .....	33
Figure 2.29	Static DGPS error in short distance measurements .....	33
Figure 2.30	Static DGPS convergence, recovery from full blockage.....	35
Figure 2.31	Close-up of static DGPS convergence.....	35
Figure 2.32	Static DGPS convergence .....	36
Figure 3.1	Dynamic DGPS accuracy experimental configuration .....	40
Figure 3.2	Camera field of view showing correction for GPS .....	41
Figure 3.3	Image of tile and survey nail as seen by camera .....	42
Figure 3.4	Data acquisition for dynamic DGPS evaluation .....	44

Figure 3.5	Dynamic error in DM and PDM .....	46
Figure 3.6	Dynamic error in DM and PDM: variance of data .....	47
Figure 3.7	Timing diagram for dynamic DGPS data acquisition .....	49
Figure 3.8	Raw DGPS dynamic error in DM .....	51
Figure 3.9	Adjusted DGPS dynamic error in DM .....	51
Figure 3.10	DGPS dynamic error PDM .....	53
Figure 3.11	Raw DGPS dynamic error vs velocity .....	55
Figure 3.12	Adjusted DGPS dynamic error vs velocity .....	55
Figure 3.13	Dynamic test: DGPS logged during 6 laps .....	57
Figure 3.14	Close-up of straight section of laps at Mn/ROAD .....	57
Figure 3.15	Close-up of northwestern curve section of laps at Mn/ROAD .....	58



## Executive Summary

The University of Minnesota, in conjunction with the Minnesota Department of Transportation, is investigating means for reducing roadway departure incidents. As part of this program, we are working on highway lane sensing strategies that can operate under road and weather conditions typical of northern climates and guidance systems which can take over control of the vehicle in case the driver becomes incapacitated.

Our experimental testbed is based on a Navistar 9400 series sleeper cab and is equipped with electronically controlled throttle, steering and brake subsystems. We are evaluating a Kalman filter used to estimate the lateral dynamics of the vehicle, which, among other variables, are determined by the vehicle's lateral velocity and yaw angular rate in vehicle coordinates (moving local coordinate system), as well as its X and Y state plane coordinates with respect to an inertial coordinate system (global coordinate system). To evaluate this concept, we rely on two different sensory systems - a second generation Differential Global Positioning System (DGPS) and an Inertial Measurement Unit (IMU). The truck's position and velocity are checked in real-time against the roadway's lane geometry as stored in a digital map. To our knowledge, this is the first evaluation of DGPS used directly for vehicle based lane sensing.

This paper documents the results of tests of the 5 Hz NovAtel RT20 DGPS receiver. Tests were conducted at the 2.4 mi. (3.86 km) Mn/ROAD pavement test facility using surveyed locations distributed around the road. In a series of 32 static tests, the overall mean for the offset errors of the DGPS determined absolute position was 0.71 cm in X and 1.19 cm in Y, with a mean standard deviation of 0.52 cm in X and 0.83 cm in Y. The mean did vary from one test to the next. The standard deviation for the mean over all runs was 3.01 cm in X and 3.98 cm in Y. In a series of dynamic tests, where the vehicle was driven around the track at speeds of 20-35 mph, once the effect of the GPS receiver's latency was removed, the DGPS determined position exhibited a mean offset error of -17.3 cm (-6.82 in) and a mean standard deviation of 25.5 cm (10.1 in) in the direction of vehicle motion. (Negative here indicates an error ahead of the vehicle's actual position and positive indicates an error lagging the vehicle's position for measurement in the direction of motion.) In the direction perpendicular to vehicle motion, the mean offset was 4.57 cm (1.8 in) with a mean standard deviation of 39.6 cm (15.6 in). All statistics are significant at the 95% level of confidence. In these tests, there were no overhead obstructions and so continuous satellite lock was possible. Tests at higher speeds are planned for the future.





# CHAPTER 1

## Introduction

Lane departures lead to many accidents each year; in particular on rural roads. Such accidents may be the result of drowsy driving, lack of visibility, or a host of other factors [1]. This paper describes technology being studied as part of a system intended to improve truck safety on rural roads. Our approach is to use in-vehicle systems which can sense the position of the vehicle and steer the vehicle to safety if it begins to run off the road [2]. Alternative highway applications of GPS such as platoon following [16] and map based navigation [17] depend completely on a driver (for platoon following on the driver of the lead vehicle) and thus do not address the problems of drowsy driving or reduced visibility.

We chose to focus on in-vehicle systems because they can operate without the substantive changes in the infrastructure required by other sensing and guidance systems such as magnetometer-based sensing [3]. We chose Differential GPS as the primary sensor modality to measure the vehicle's position on the road in Minnesota state plane or county coordinates. A major advantage GPS has over other sensing technologies, such as computer vision [4],[12], is that it can be operated under all visibility and road conditions, including times when roads are covered by snow. A sensing system which exhibits many of the same advantages as GPS is Loran C. However, Loran C uses land-based radio location technology first developed by the Coast Guard [14],[15]. Loran C can only achieve 10 meter resolution.

In order to compensate for the limitations of GPS, an Inertial Measurement Unit is also used. This second suite of sensors includes two angular rate sensors (gyros) (Andrew Corporation) measuring yaw and roll rates, two accelerometers (Allied Signal, Inc.) for measuring lateral and longitudinal accelerations, and one three axis magnetometer (Watson Industries, Inc.). The reason for using this second group of sensors is primarily due to their higher data bandwidth and robustness of operation as opposed to the available data acquisition rate of GPS position (5 Hz) and to the potential unavailability of GPS signals caused by poor satellite constellation, blockage of receiver, etc. On the other hand, GPS provides a sensing medium that is not subject to the long term drift that is typically associated with inertial measurements and can therefore be used to provide absolute position corrections.

Our approach to prevent road departure through in-vehicle sensing and control is to use Kalman filter theory to integrate the two groups of sensors described above (GPS and IMU). Galijan et al. [5] extensively examined the applicability of GPS to vehicle motion sensing

applications. Applications of Kalman filter techniques to various vehicle control and tracking projects (including the Automated Highway System (AHS)) have drawn considerable attention in recent years. Da and Dedes [6], and He [7] for example, attempt to integrate GPS with INS by using a Kalman filter in which GPS data is used to update the INS system. Other similar guidance methodologies have been reported in the literature [8], [9], [10]. The approach that we are taking towards integration of the two sensor groups differs in that we are using two different Kalman filters. One is associated with the IMU and the other with the GPS system. The implementation of these two Kalman filters is obtained by using an experimentally validated lateral dynamic model of the experimental vehicle that includes tire dynamics and a dynamic model that describes the differential kinematics of the vehicle's motion. These dynamic models are associated with the IMU and the GPS Kalman filters respectively. During the times when GPS data is not available, the Kalman filter associated with the IMU provides filtered data of quantities local to the vehicle, i.e., lateral and forward velocity, yaw rate, etc. These measurements are then used to update the position of the vehicle in Minnesota state plane or county coordinates through the differential kinematics relationships.

In this paper we focus on the evaluation of the DGPS system. The purpose of this evaluation is twofold. First, we wish to know how well DGPS functions as a sensor for supporting vehicle tracking, in terms of accuracy, repeatability and robustness (e.g., is DGPS accurate enough to track the vehicle in its lane on straight-aways and while maneuvering curves at various speeds? Is it sufficiently accurate to detect imminent lane departure for warning systems?). Second, we wish to evaluate the sensors' properties (such as the covariance matrix) needed by the Kalman filter. At the same time we have been seeking ways of improving the DGPS data during motion by correcting them through the use of signals available from the IMU.

The Global Positioning System (GPS) is a system of 24 satellites which transmits real-time signals which are then used to triangulate the position of a GPS receiver. The satellites orbit the globe every 12 hours and transmit accurately timed, coded pulses to the Earth. The satellite orbits are such that there are always at least six satellites above the horizon. Using four or more satellites, a GPS receiver determines its position in latitude, longitude and height above sea level by solving a series of equations based on the number of satellites available. The accuracy of the position can be degraded by many factors, such as corruption of broadcast, poor satellite arrangement in the sky, distortion due to the ionosphere, and Doppler shift caused by the satellite's motion [5],[13]. These errors can be greatly reduced or eliminated through the use of Differential GPS (DGPS).

DGPS uses two GPS receivers and a differential correction receiver. One GPS receiver along with the differential antenna is on the object or vehicle which is to be tracked (receiver A), and the other GPS receiver is mounted in a nearby surveyed location (receiver B).

During operation, since the receivers are close to one another, the errors in the signals that they simultaneously receive from the satellites at any instant in time are almost identical. Thus, knowing the error at one receiver means knowing the error at the other receiver. After each position signal is received, Receiver B calculates the difference between its received position and its surveyed position. It then transmits this error correction value to receiver A in real time. Receiver A is thus able to compute its position much more accurately.

Many DGPS systems are commercially available. We evaluated a DGPS system based on the NovAtel RT20, which was chosen because its specifications indicated errors on the order of centimeters, a latency of 70 ms and a data acquisition rate of 5 Hz [25]. According to the vendor, the system reaches an accuracy of 20 cm (7.87 in) C.E.P. after the first few minutes of operation with further improvements in accuracy taking place over time (see Figure 1.1). (The conversion from C.E.P. to standard deviation is described in [11].) The results we obtained in our experiments described below, indicate potential accuracy's higher than those reported by others thus far [8],[9],[10].

We tested the DGPS system on a Navistar 9400 series semi tractor at the Mn/ROAD pavement research facility's low volume test track in Wright County, MN. The Mn/ROAD track is a two-lane, 3.86 km (2.4 mi) road in a race track configuration, as shown in Figures 1.2 and 1.3. Survey markers are embedded in the Mn/ROAD track every 30.48 m (100 ft). The surveyed accuracy of the survey nail locations is  $\pm 6$  cm in longitude and  $\pm 3$  cm in latitude (as per the Surveying and Mapping Section, Mn/DOT). We used the survey nails as the "ground truth" against which to test the accuracy of the DGPS system. (Note that there are abrupt changes in the numbering sequence at both ends of the track. The breaks occur between survey nails 48 and 160 on the northwestern end and between survey nails 108 and 230 on the southeastern end.). The differential base (i.e. the GPS antenna providing correction signals) was mounted on the roof of the research building at the site (see Figure 1.4).

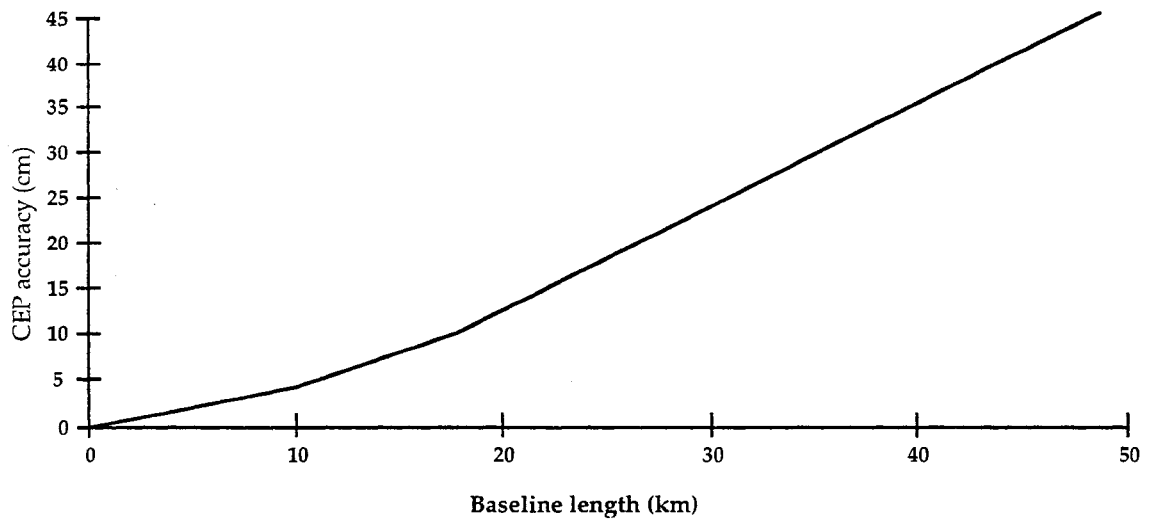
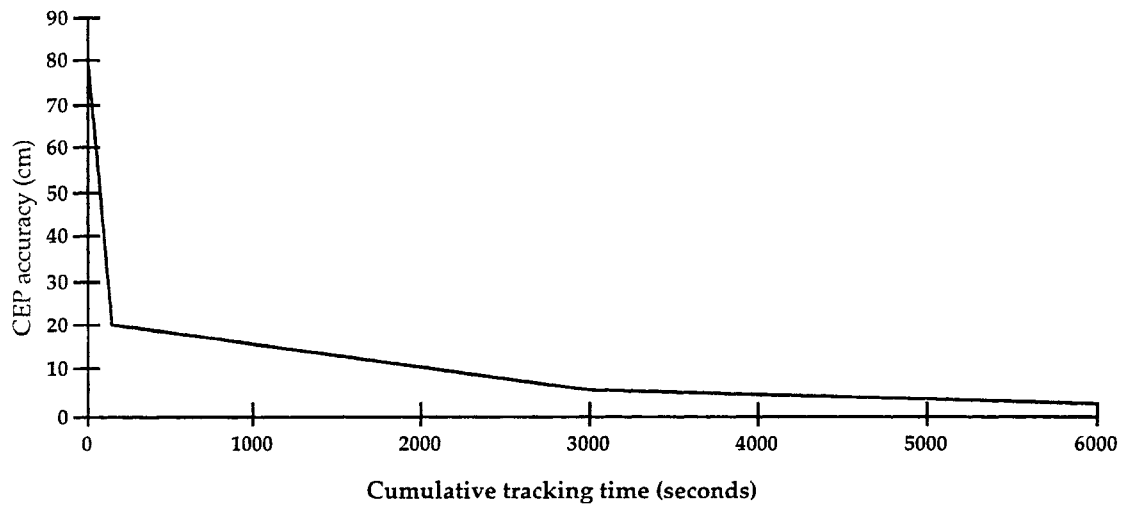


Figure 1.1 NovAtel RT20 DGPS accuracy specifications as per the vendor (Note that 5 cm CEP accuracy is achieved after 50 min (3000 sec) of lock.)

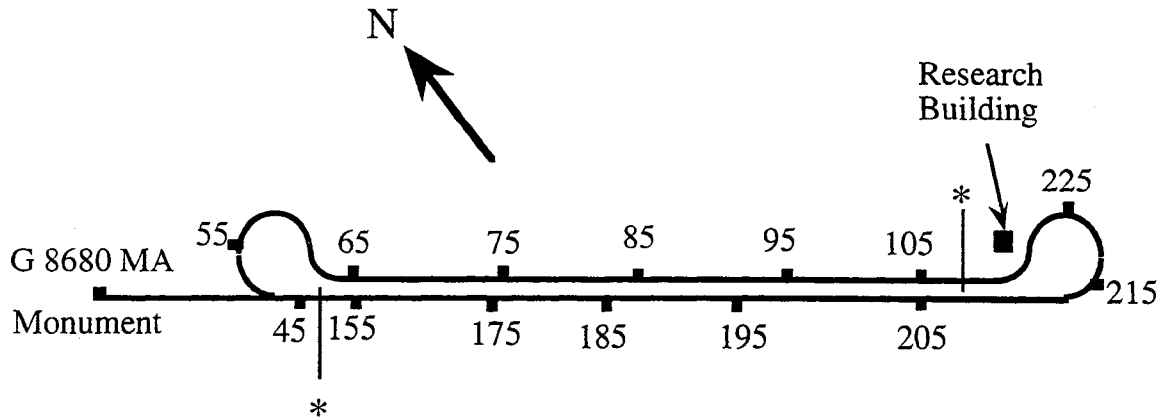


Figure 1.2 Mn/ROAD test facility (Wright County, MN) showing survey nail locations and geodetic monument (Not to scale.)  
 (\* There is a break in the sequence between 108 and 230 at the southeastern end and between 48 and 160 at the northwestern end.)

The set of experiments discussed below were conducted to determine the position accuracy and repeatability of the NovAtel DGPS system with the GPS receiver antenna mounted on the Navistar truck. Experiments were conducted while the truck was stopped (static results) and while moving between 20 and 35 miles per hour (dynamic results).



Figure 1.3 Aerial photograph of Mn/Road track



Figure 1.4 Research building at Mn/ROAD site.  
(The differential GPS antenna is situated on the right corner  
of the roof above.)

## CHAPTER 2

### Evaluation of Static Performance

#### *Description of Experiment*

The static GPS experiments were conducted in order to determine the position accuracy and repeatability of the NovAtel DGPS system [22] while the GPS receiver antenna was stationary.

The computer and GPS receiver were powered via an uninterruptible power supply hooked up to two 12 volt batteries which were in turn connected to the truck's alternator. The GPS receiver antenna and the antenna for receiving the differential corrections were both mounted on top of the cab's sleeper section (10 feet above the ground). The receiver antenna was suspended one foot off to the side of the cab (see Fig. 2.1). The GPS receiver was connected to the computer through a serial communications port. For the static DGPS experiments, software provided by NovAtel (WinSat v. 1.01, Copyright NovAtel Communications Ltd., 1993,1994, run under Windows v. 3.1 on a 486 computer) was used to record the DGPS position logs. Each daily session of experiments began by locking the DGPS system on to the satellites. The system was first run for approximately 60 minutes, allowing time for the position solution calculations of the DGPS system to converge to a solution within our desired range. In a final truck based implementation of a system used for road departure prevention, it would not be unreasonable for the GPS receiver to be left on all the time.

For the static experiments, the truck was parked on the shoulder such that the GPS antenna was within a few inches of the survey nail in the horizontal projection plane of the road. However, since absolute accuracy in positioning the truck and the attached GPS antenna over a survey nail was nearly impossible, we used a plumb bob and measurement grid to measure a correcting offset.

The grid would be laid on the road above the survey nail and aligned with North using a compass. The distances between the plumb bob (GPS antenna) and the survey nail could be read directly along the north and east directions.

Once the offsets between the survey nail and GPS antenna were recorded, the computer logged the DGPS position data for approximately 3 minutes at a rate of 5 Hz (approximately 800 data points collected). This process was repeated multiples times at each survey nail during three different test sessions to determine the absolute accuracy of the static DGPS system. We also used this process to make relative distance measurements between points on the track during 3 different test sessions (see Relative Accuracy section below).

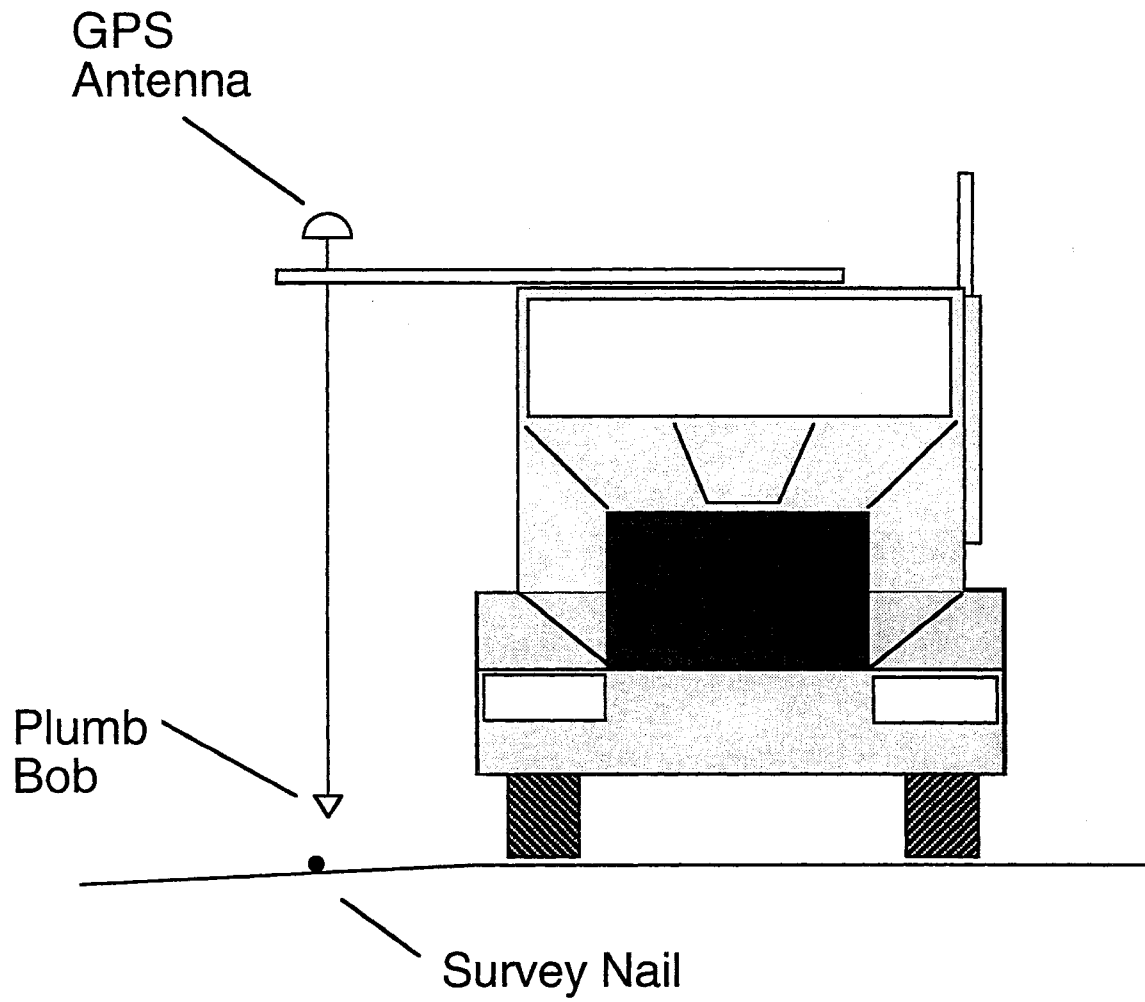


Figure 2.1 Static DGPS accuracy experimental configuration  
(Not to scale.)



## *Results*

### *Absolute Position Accuracy*

Before the collected data could be analyzed, it was converted from the NGS (National Geodetic Survey) format generated by the GPS system (decimal degrees of latitude and longitude) into the county coordinates (Wright County, MN) in which the survey nail locations were surveyed (see [18],[20],[26], and Appendix A).

During each session, we tested the accuracy of the DGPS system at 5 to 8 survey nails. At each nail we collected data for approximately 3 minutes. To test the repeatability of the system, we made multiple tests at each nail during the same day and on different days. In all, we ran a total of 32 test runs over 3 different testing dates. In the following analysis, we compare static DGPS accuracy at different survey nail locations during the same run of tests on a single day, at the same survey nail location during different runs on a single day, and at the same survey nail location on different days.

A data set was collected for approximately 3 minutes (at 5 Hz) at each survey nail. Each data set has its own mean and standard deviation in both the X and Y directions, as well as its own covariance matrix in X and Y. In the coordinate system, positive X is defined as east and positive Y is defined as north. The exact equations that were used to compute these statistics are summarized in Appendix D.

The absolute accuracy of the DGPS system was measured in terms of offset errors using (1) the overall mean for all 32 tests, (2) the amount that the mean changed between tests (standard deviation of the mean), and (3) the standard deviation about each test's mean. These statistics are illustrated in Figure 2.2. The overall mean for the offset errors of the DGPS determined absolute position was 0.71 cm in X and 1.19 cm in Y. The standard deviation about each test's mean was 0.52 cm in X and 0.83 cm in Y. The value of the overall mean of all runs is misleading because the mean did vary from one test to the next. The standard deviation for the mean over all 32 tests was 3.01 cm in X and 3.98 cm in Y.

We calculated confidence intervals for the means of all the data sets at the 95% level of confidence to ensure statistical significance. These confidence intervals were calculated using the approximately 800 data points taken over 3 minutes during each run. We also calculated similar confidence intervals for the ensemble means. These confidence intervals were calculated using the number of data sets being compared i.e., if four runs were taken at the same nail, then the number

of data sets for that ensemble would be four. All of the data presented is statistically significant at the 95% level of confidence.

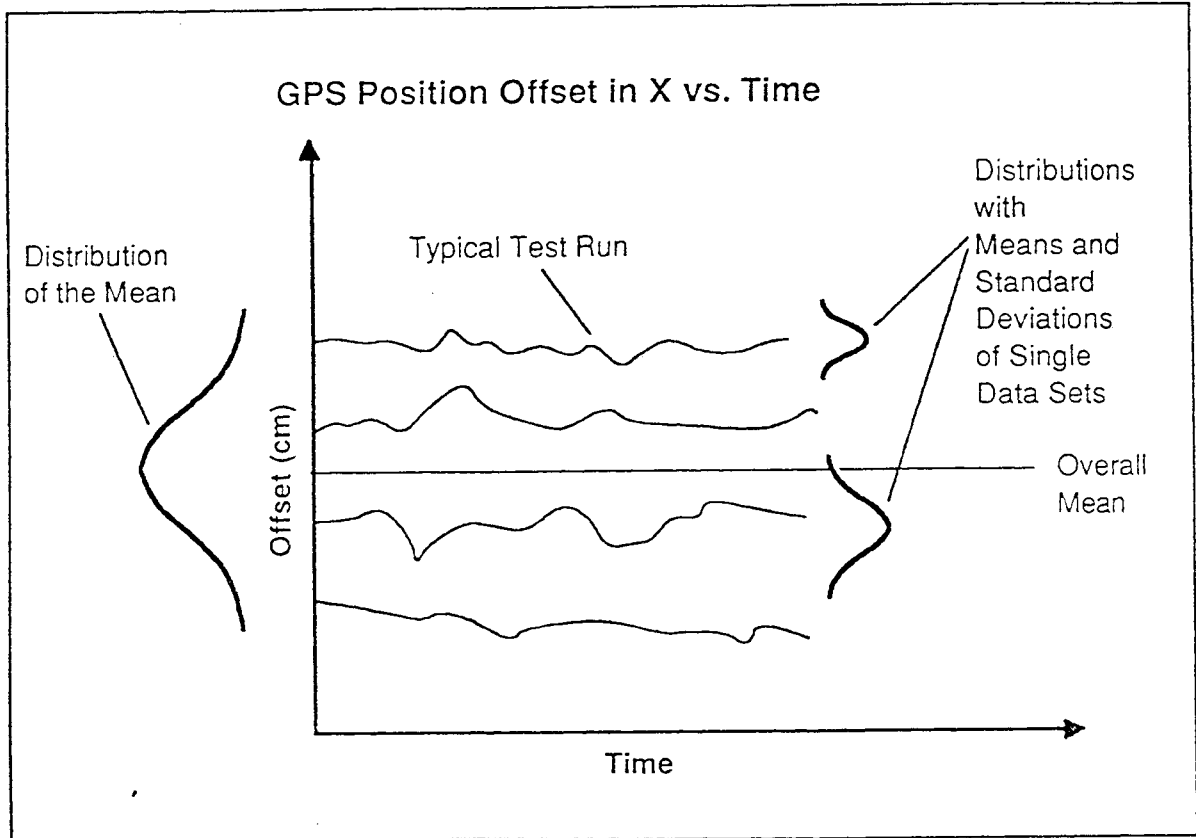


Figure 2.2 Pictorial representation of statistical terminology

*Comparison of Static DGPS Accuracy During a Single Test Run*

Figures 2.3 and 2.4 show static DGPS position readings in X and Y at four survey nails during run 1 on 9/26/95. The results are summarized in Table 2.1.

The covariance matrices for the experimental data were found to be relatively consistent for different locations around the Mn/ROAD site. We found that the variance in the Y direction was consistently higher than the variance in the X direction for all four survey nails, while (xy was rather small, suggesting that the X and Y results were not statistically coupled.

Table 2.1 Static DGPS Accuracy During a Single Test Run

	<b>Nail 63</b>	<b>Nail 90</b>	<b>Nail 101</b>	<b>Nail 175</b>
<b>Mean X offset</b>	0.92 cm (0.36 in)	0.83 cm (0.33 in)	3.89 cm (1.53 in)	2.72 cm (1.07 in)
<b>Mean Y offset</b>	0.91 cm (0.36 in)	2.48 cm (0.98 in)	0.64 cm (0.25 in)	3.70 cm (1.46 in)
<b>X std. dev.</b>	0.42 cm (0.16 in)	0.49 cm (0.19 in)	0.47 cm (0.19 in)	0.49 cm (0.19 in)
<b>Y std. dev.</b>	0.66 cm (0.26 in)	0.73 cm (0.29 in)	0.87 cm (0.34 in)	0.61 cm (0.24 in)
<b>Cov 63 (cm*cm)</b>		<b>X</b>	<b>Y</b>	
	<b>X</b>	0.175	0.033	
	<b>Y</b>	0.033	0.439	
<b>Cov 90 (cm*cm)</b>		<b>X</b>	<b>Y</b>	
	<b>X</b>	0.24	0.033	
	<b>Y</b>	0.033	0.537	
<b>Cov 101 (cm*cm)</b>		<b>X</b>	<b>Y</b>	
	<b>X</b>	0.221	0.162	
	<b>Y</b>	0.162	0.76	
<b>Cov 175 (cm*cm)</b>		<b>X</b>	<b>Y</b>	
	<b>X</b>	0.239	0.017	
	<b>Y</b>	0.017	0.366	
<b>Overall mean in X direction</b>	2.09 cm (0.82 in)		<b>X standard deviation of the mean</b>	
			1.53 cm (0.60 in)	
<b>Overall mean in Y direction</b>	1.93 cm (0.76 in)		<b>Y standard deviation of the mean</b>	
			1.56 cm (0.61 in)	

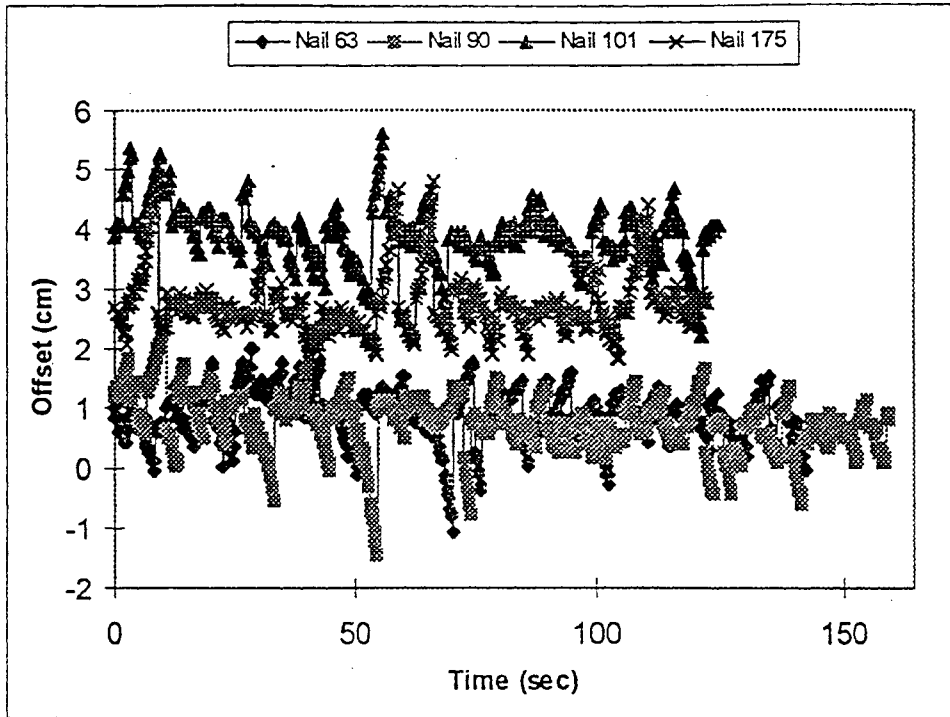


Figure 2.3 9/26/95 Static DGPS X offset from true at four survey nails (5 samples/sec collected).

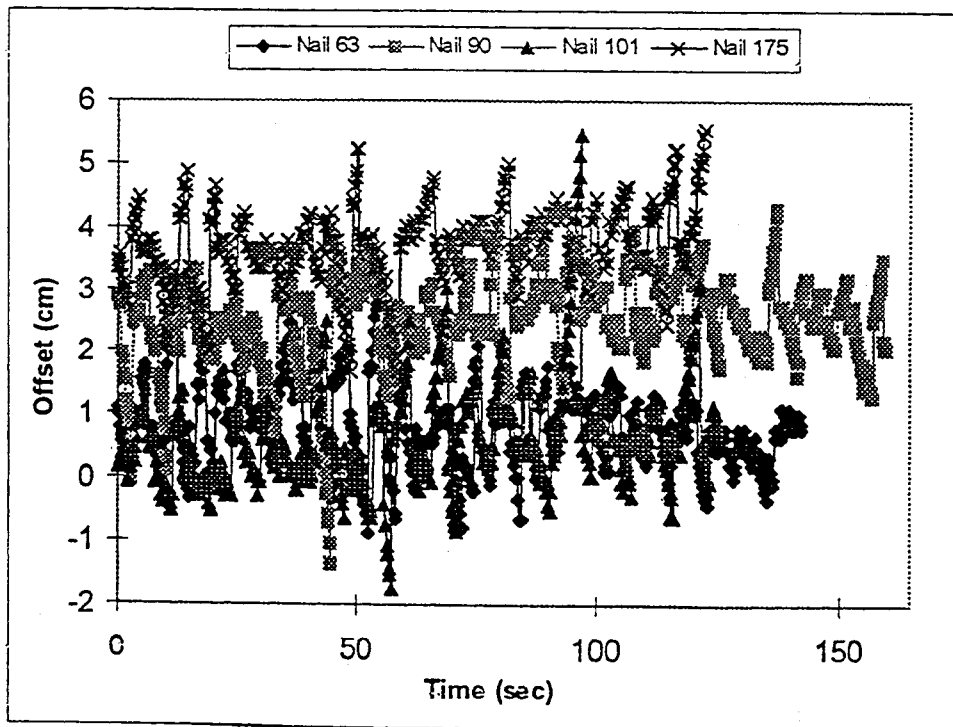


Figure 2.4 9/26/95 Static DGPS Y offset from true at four survey nails (5 samples/sec collected).

The value of the ensemble standard deviation mainly depends on the “drift” in mean offset amongst the runs, since the data in each run varies little from its mean. This drift may be explained by the oscillatory behavior of the position readings of the DGPS (described in Section 2.2.1 below).

We cannot measure the absolute accuracy of our results any better than the accuracy level to which the nails were originally surveyed ((6 cm in the X direction (longitude) and (3 cm in the Y direction (latitude)). Whatever error exists due to the survey inaccuracy is of course constant, so we should be able to obtain repeatable results at the same survey nail over many test runs. However, we see below that this is not the case. We believe that drifts in the mean errors are due to the “oscillatory” behavior in the position readings of DGPS system that we observed. This oscillatory behavior was discovered during the 13 day static test described below.

The results that follow are surprisingly accurate given these two sources of uncertainty - (1) the error associated with the survey nail data and (2) the oscillatory drift in the GPS data. Our results indicate that the accuracy of the GPS readings are at least of the same order as the surveyed nails that we used as “ground truth.”

#### *Static DGPS Accuracy at Individual Survey Nails*

Figures 2.5 - 2.12 show single runs at survey nails 63, 90, 101 and 175. The graphs show the static DGPS offset and the running standard deviation for each nail. Running standard deviations are computed continuously based on the previous 25 samples (5 seconds of data). The results for these survey nails are summarized in Table 2.1.

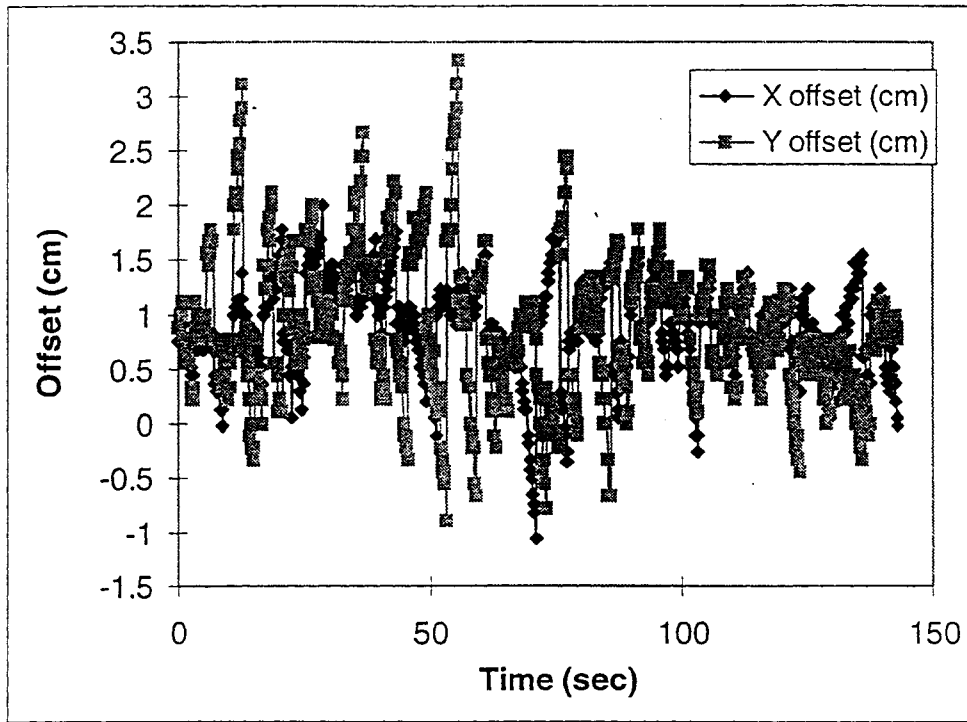


Figure 2.5 9/26/95 Survey nail 63 DGPS offset from true (5 samples/sec collected).

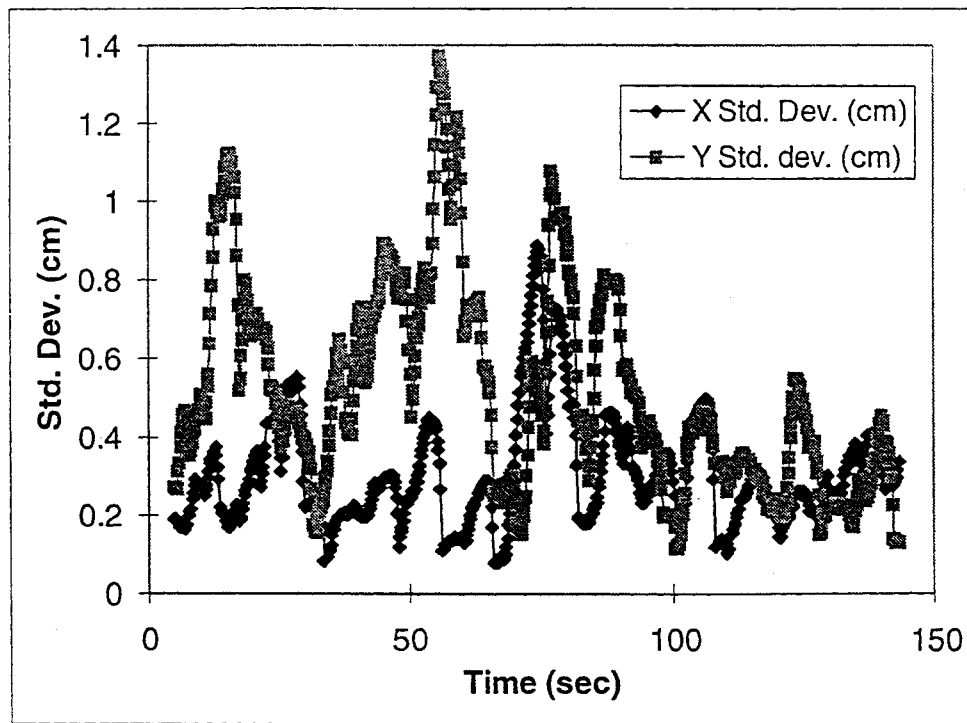


Figure 2.6 9/26/95 Survey nail 63 DGPS running 25 pt standard deviation

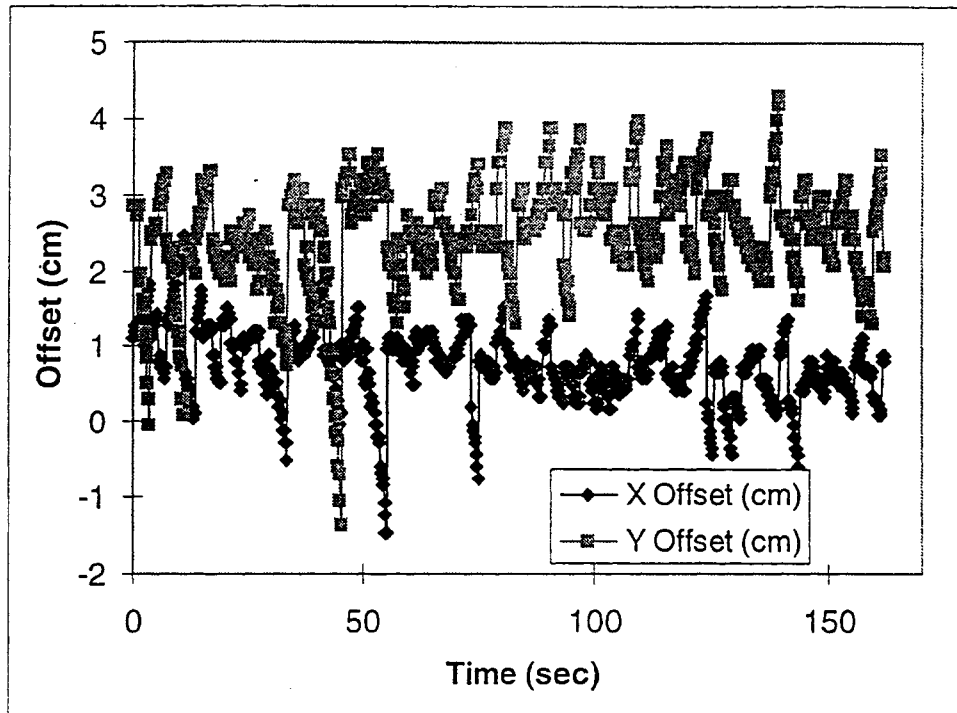


Figure 2.7 9/26/95 Survey nail 90 DGPS offset from true (5 samples/sec collected).

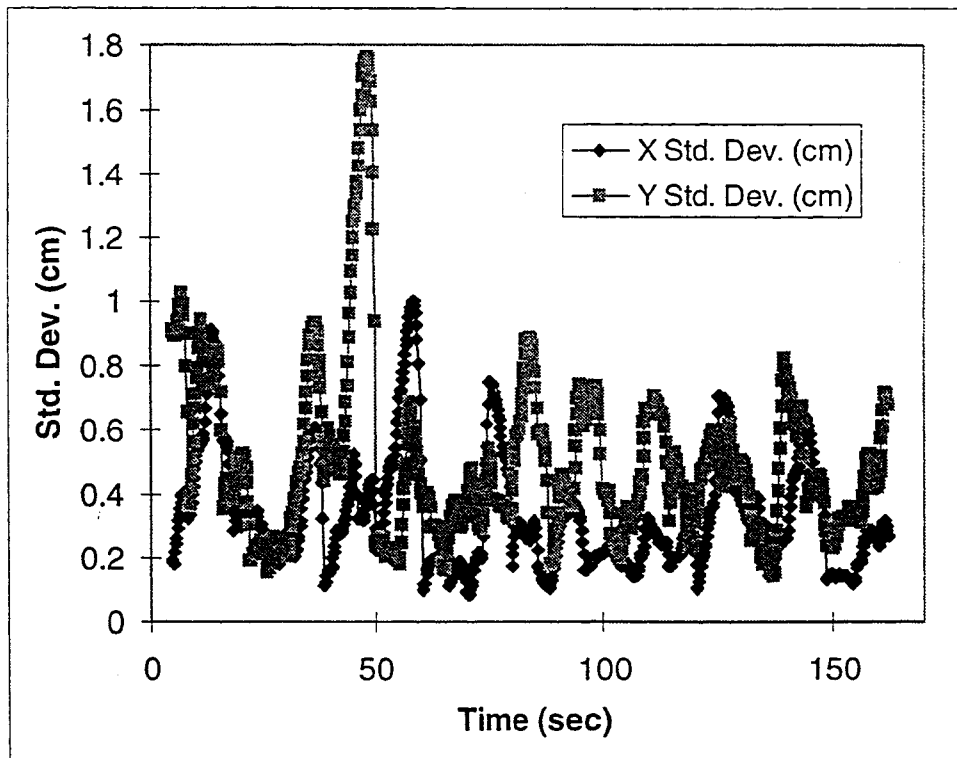


Figure 2.8 9/26/95 Survey nail 90 DGPS running 25 pt standard deviation

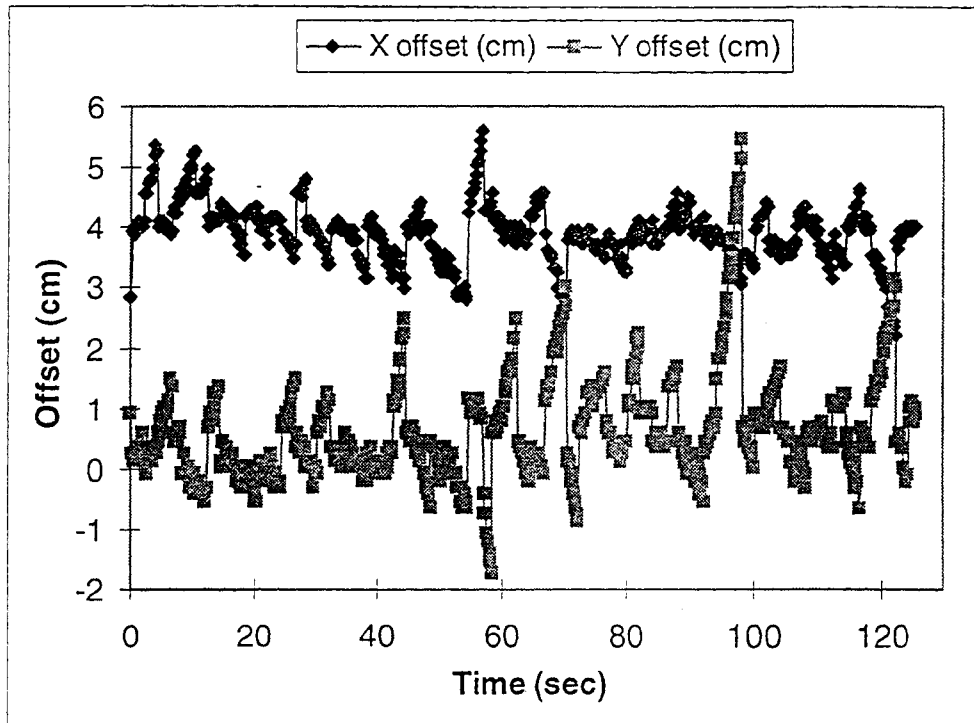


Figure 2.9 9/26/95 Survey nail 101 DGPS offset from true (5 samples/sec collected).

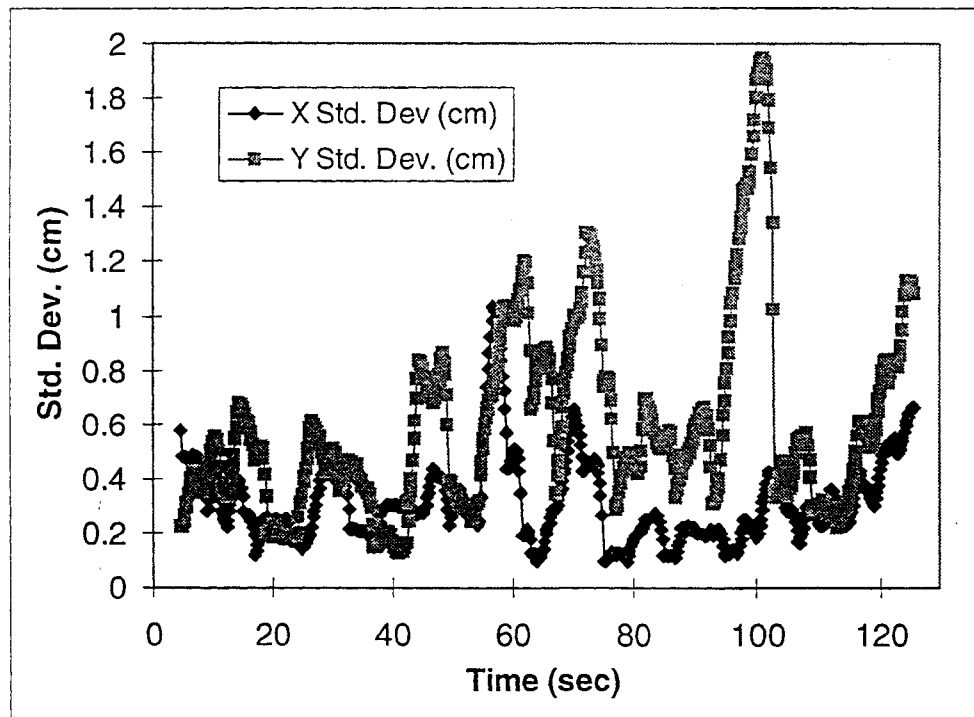


Figure 2.10 9/26/95 Survey nail 101 DGPS running 25 pt standard deviation



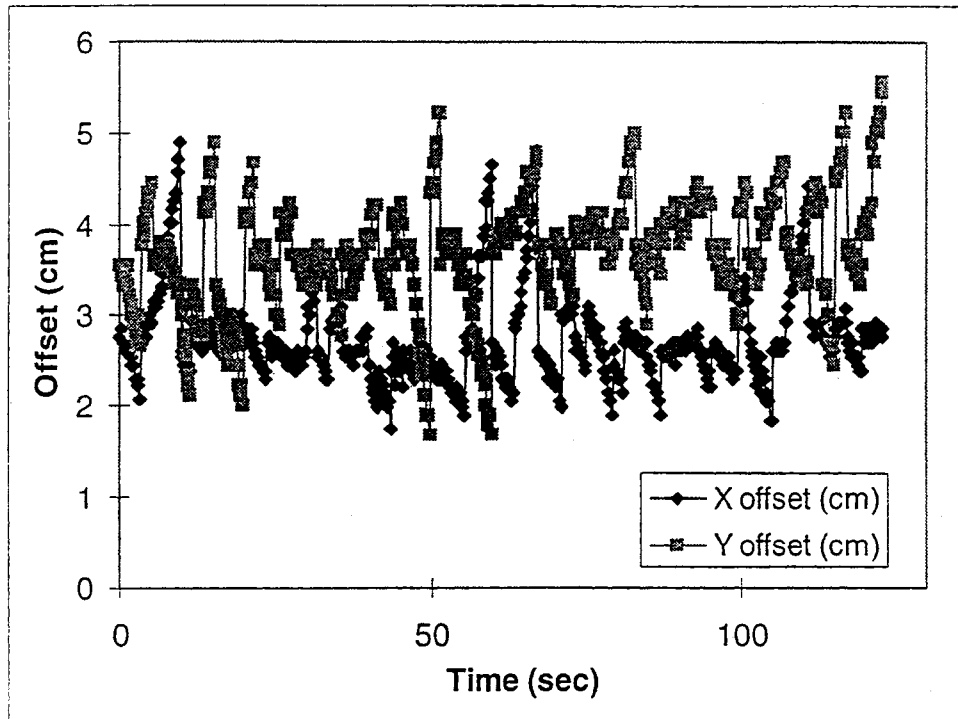


Figure 2.11 9/26/95 Survey nail 175 DGPS offset from true (5 samples/sec collected).

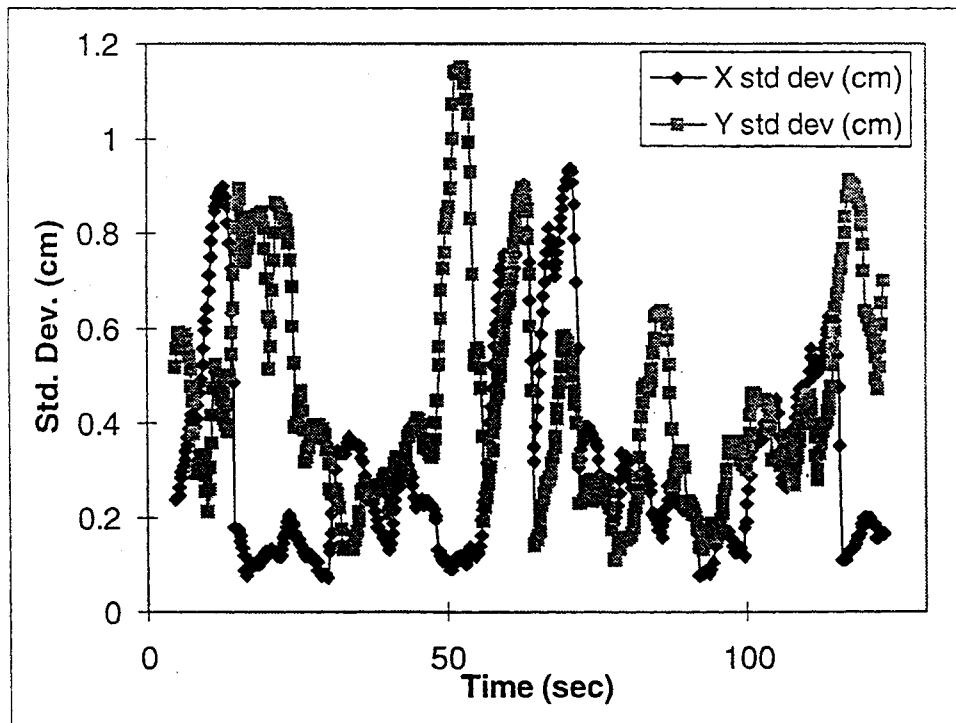


Figure 2.12 9/26/95 Survey nail 175 DGPS running 25 pt standard deviation

*Comparison of Static DGPS Accuracy at the Same Survey Nail*

Figures 2.13 and 2.14 show the static DGPS results at survey nail 63 during two runs taken an hour apart. Figures 2.15 and 2.16 show similar results for survey nail 90. Surprisingly, changes of almost 4 cm are seen in the offsets between two tests taken only an hour apart. The results of these tests are summarized in Table 2.2 below.

Table 2.2 Static DGPS Accuracy at the Same Nail on the Same Day

<u>Nail 63</u>					
<u>Run 1</u>					
Mean X offset	X std. dev.	Cov run 1 (cm*cm)	X	Y	
-0.83 cm (-0.33 in)	0.47 cm (0.19 in)	X	0.224	0.009	
Mean Y offset	Y std. dev.	Y	0.009	0.483	
2.12 cm (0.83 in)	0.69 cm (0.27 in)				
<u>Run 2</u>					
Mean X offset	X std. dev.	Cov run 2 (cm*cm)	X	Y	
0.98 cm (0.39 in)	0.65 cm (0.26 in)	X	0.424	0.492	
Mean Y offset	Y std. dev.	Y	0.492	1.215	
0.39 cm (0.15 in)	1.10 cm (0.43 in)				
<u>Nail 90</u>					
<u>Run 1</u>					
Mean X offset	X std. dev.	Cov run 1 (cm*cm)	X	Y	
-0.45 cm (-0.18 in)	0.49 cm (0.19 in)	X	0.239	0.104	
Mean Y offset	Y std. dev.	Y	0.104	0.509	
2.36 cm (0.93 in)	0.71 cm (0.28 in)				
<u>Run 2</u>					
Mean X offset	X std. dev.	Cov run 2 (cm*cm)	X	Y	
2.32 cm (0.91 in)	0.42 cm (0.17 in)	X	0.174	0.141	
Mean Y offset	Y std. dev.	Y	0.141	0.757	
-0.82 cm (-0.32 in)	0.87 cm (0.34 in)				

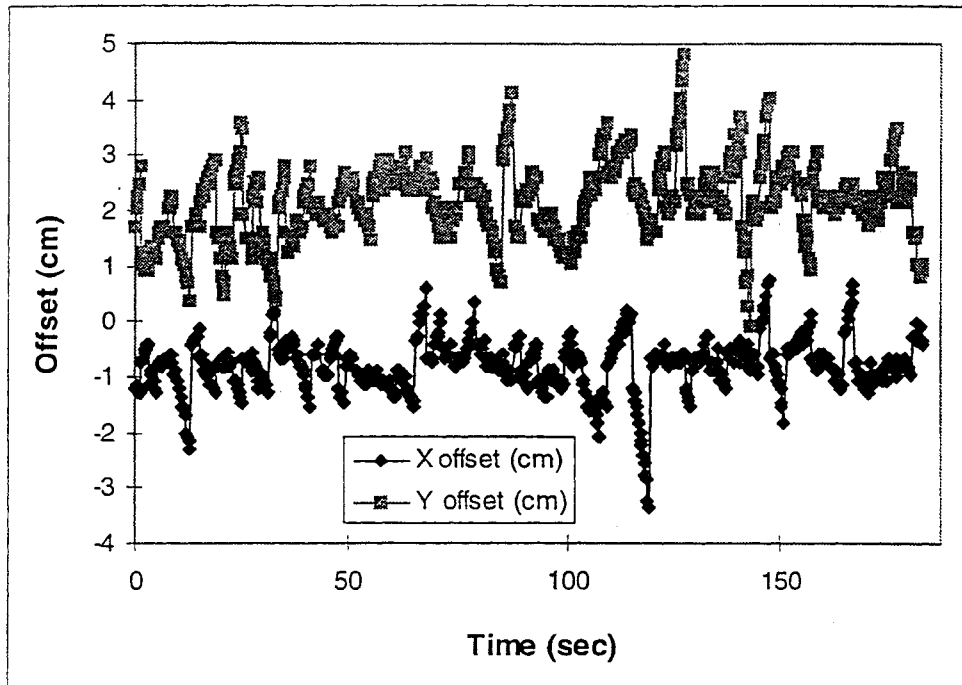


Figure 2.13 11/09/95 Static DGPS offset from true at nail 63, run 1

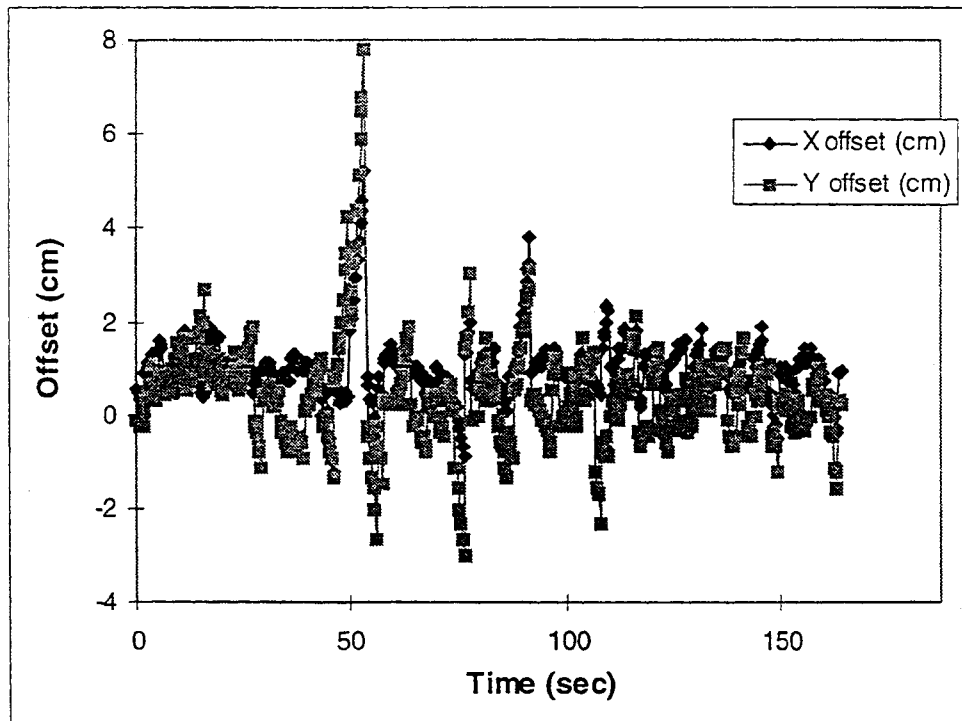


Figure 2.14 11/09/95 Static DGPS offset from true at nail 63, run 2 (approx. 1 hr. after run 1)

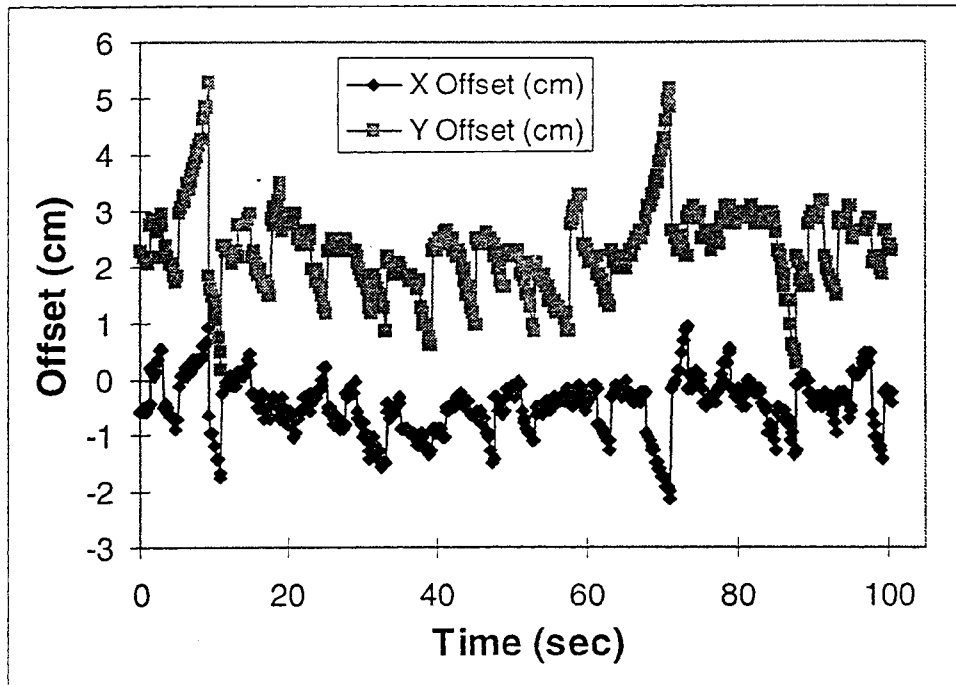


Figure 2.15 10/26/95 Static DGPS offset from true at nail 90, run 1

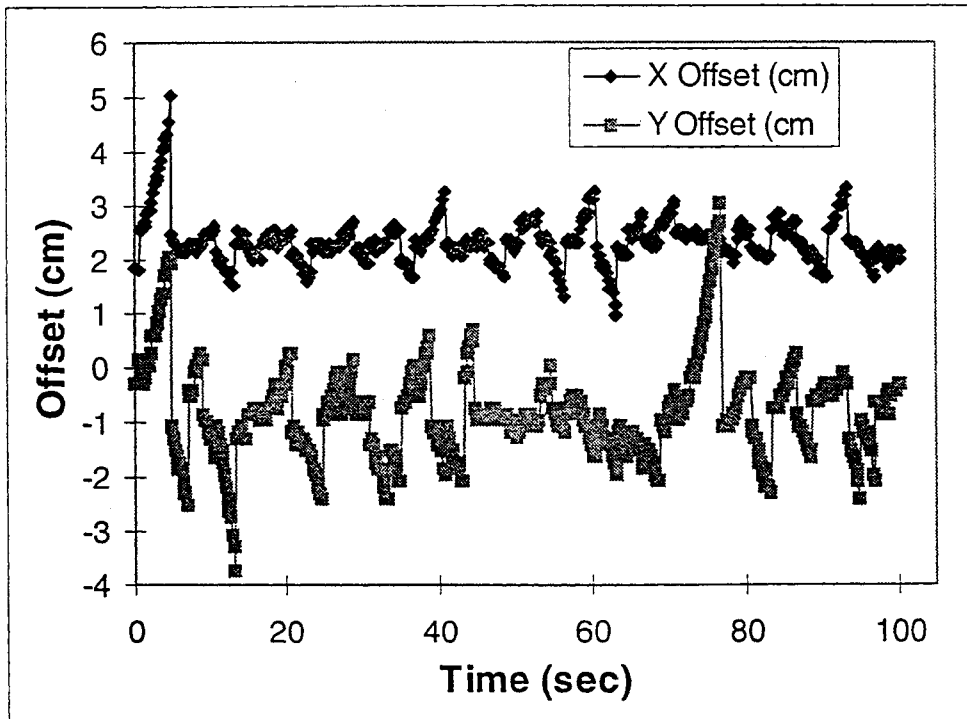


Figure 2.16 10/26/95 Static DGPS offset from true at nail 90, run 2 (approx. 1 hr. after run 1)

Figures 2.17 and 2.18 show the static DGPS results at survey nail 101 during two runs taken 14 days apart. Figures 2.19 and 2.20 show similar results for survey nail 219. Notice the change seen in the offsets between the different days. The results of these tests are summarized in Table 2.3 below. These results indicate that the variations seen between runs taken 1 hour apart are approximately the same as those for runs taken weeks apart.

Table 2.3 Static DGPS Accuracy at the Same Nail on Different Days

<u>Nail 101</u>				
<u>10/26/95</u>				
Mean X offset	X std. dev.	Cov day 1 (cm*cm)	X	Y
0.97 cm (0.381 in)	0.52 cm (0.20 in)	X	0.265	0.174
Mean Y offset	Y std. dev.	Y	0.174	0.497
2.16 cm (0.85 in)	0.71 cm (0.28 in)			
<u>11/9/95</u>				
Mean X offset	X std. dev.	Cov day 2 (cm*cm)	X	Y
-2.91 cm (-1.15 in)	0.38 cm (0.15 in)	X	0.362	0.110
Mean Y offset	Y std. dev.	Y	0.110	1.108
-2.54 cm (-1.0 in)	1.05 cm (0.41 in)			
<u>Nail 219</u>				
<u>10/26/95</u>				
Mean X offset	X std. dev.	Cov day 1 (cm*cm)	X	Y
-1.12 cm (-0.44 in)	0.64 cm (0.25 in)	X	0.407	0.165
Mean Y offset	Y std. dev.	Y	0.165	0.776
0.70 cm (0.28 in)	0.88 cm (0.35 in)			
<u>11/9/95</u>				
Mean X offset	X std. dev.	Cov day 2 (cm*cm)	X	Y
0.70 cm (0.28 in)	0.44 cm (0.17 in)	X	0.189	0.039
Mean Y offset	Y std. dev.	Y	0.039	0.542
2.95 cm (1.16 in)	0.74 cm (0.29 in)			

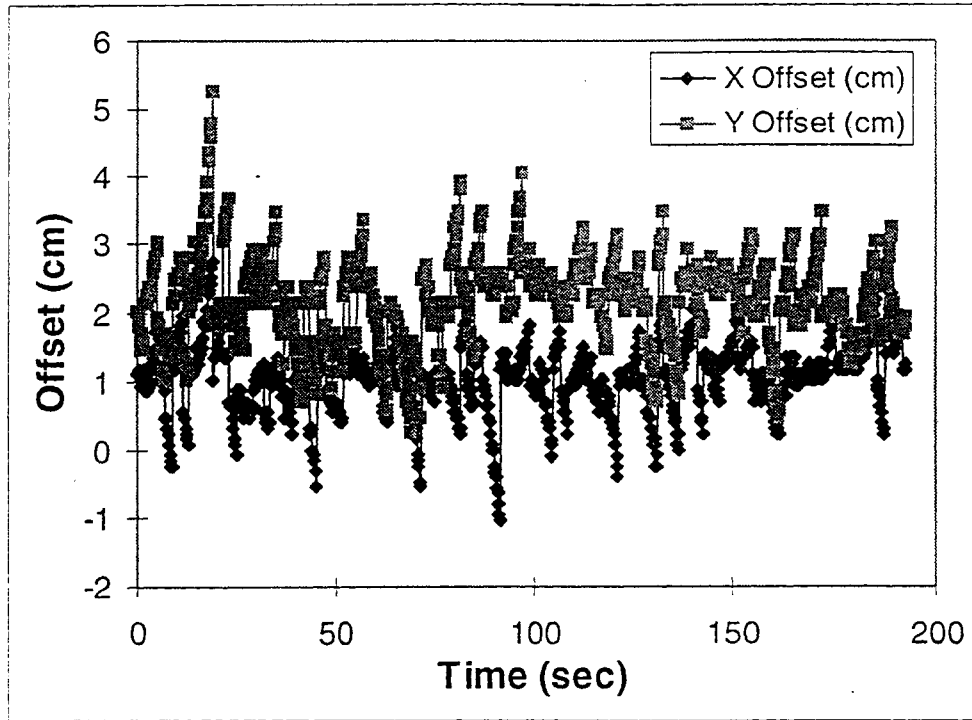


Figure 2.17 10/26/95 Static DGPS offset from true at nail 101, run 1

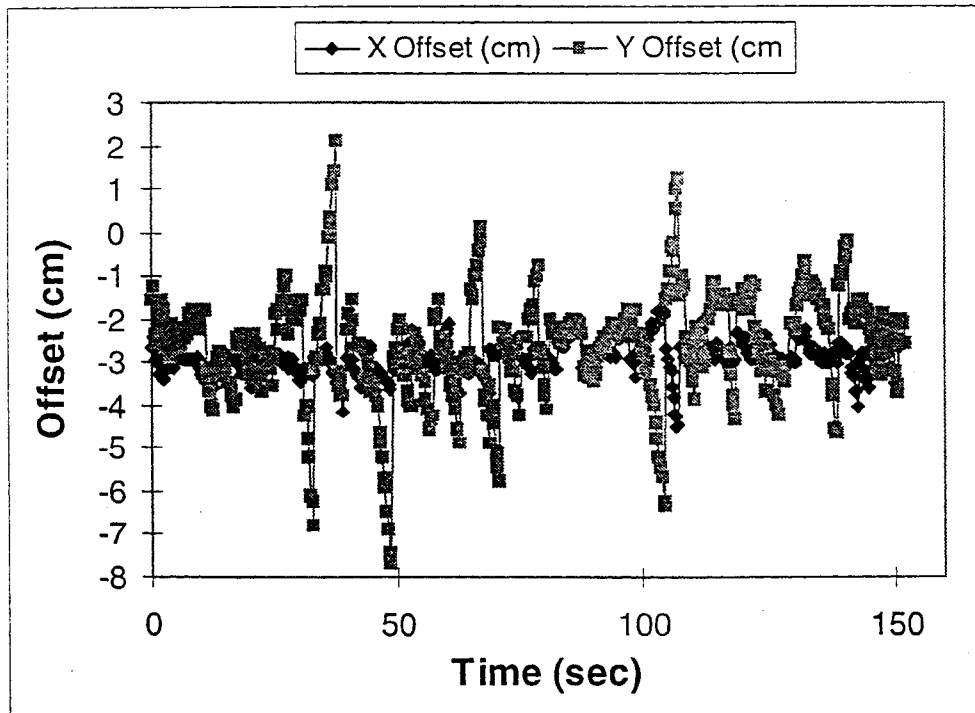


Figure 2.18 11/09/95 Static DGPS offset from true at nail 101, run 3  
(14 days after Figure 21)

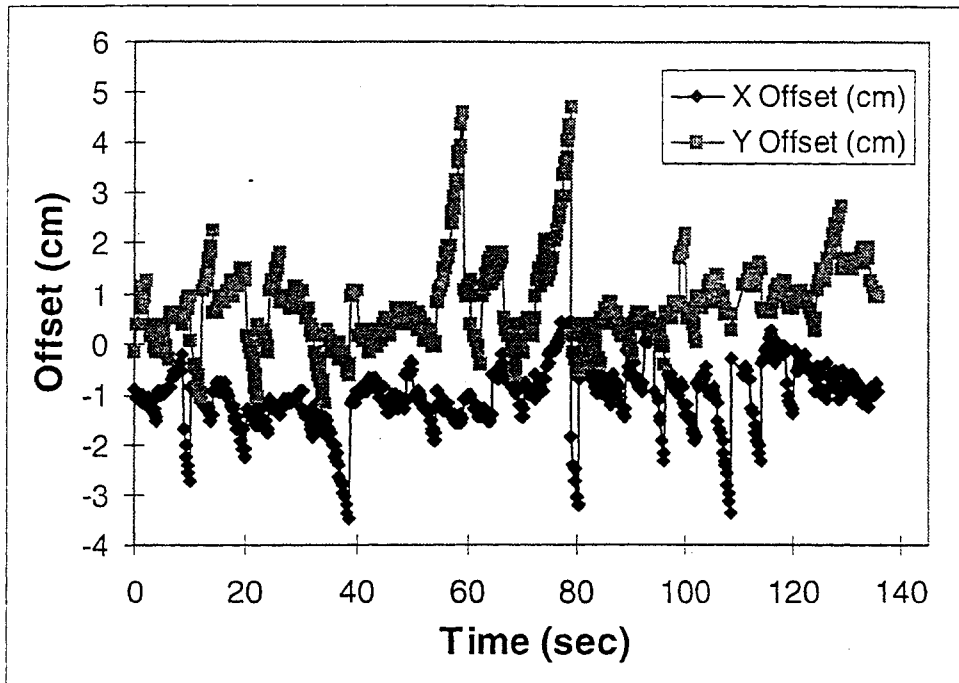


Figure 2.19 10/26/95 Static DGPS offset from true at nail 219, run 1

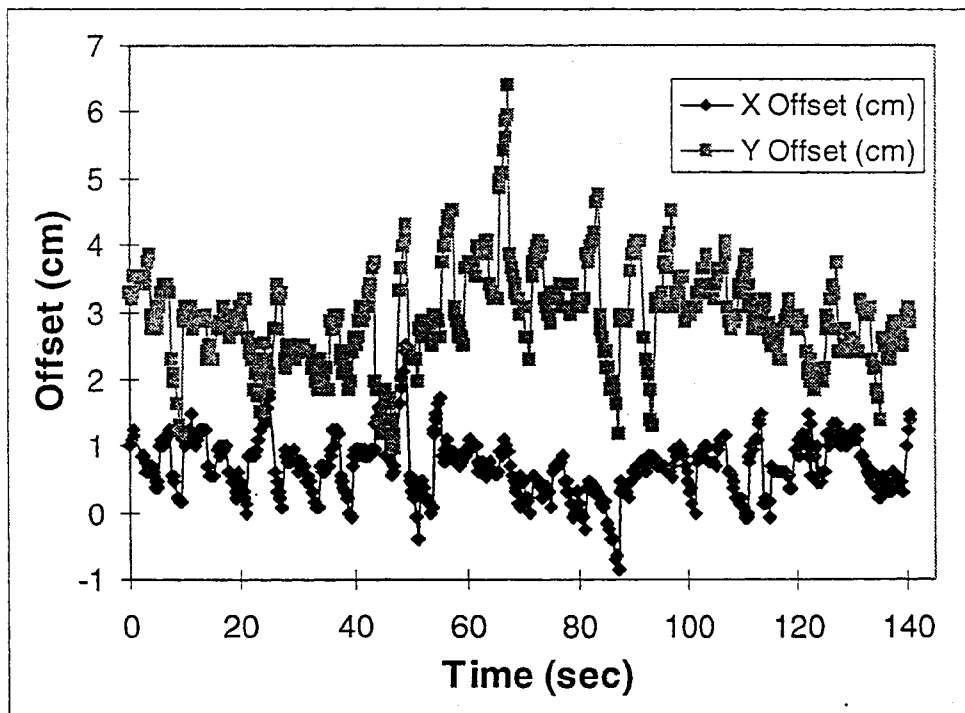


Figure 2.20 11/09/95 Static DGPS offset from true at nail 219, run 1  
(14 days after run Figure 23)

We calculated ensemble statistics for many survey nails, taking into account all of the 6 test runs taken at each nail during all 3 of the test sessions. These results are listed in Table 2.4.

Table 2.4 Ensemble Statistics

	<b><u>Nail 63</u></b>
<b>Overall mean in X direction</b> -0.06 cm (-0.024 in)	<b>Standard deviation of the mean in X</b> 1.02 cm (0.40 in)
<b>Overall mean in Y direction</b> 1.21 cm (0.48 in)	<b>Standard deviation of the mean in Y</b> 1.19 cm (0.47 in)
	<b><u>Nail 90</u></b>
<b>Overall mean in X direction</b> 0.94 cm (0.37 in)	<b>Standard deviation of the mean in X</b> 1.96 cm (0.77 in)
<b>Overall mean in Y direction</b> 0.77 cm (0.30 in)	<b>Standard deviation of the mean in Y</b> 2.26 cm (0.89 in)
	<b><u>Nail 101</u></b>
<b>Overall mean in X direction</b> -0.25 cm (-0.098 in)	<b>Standard deviation of the mean in X</b> 1.73 cm (0.68 in)
<b>Overall mean in Y direction</b> -0.19 cm (-0.075 in)	<b>Standard deviation of the mean in Y</b> 3.32 cm (1.33 in)
	<b><u>Nail 219</u></b>
<b>Overall mean in X direction</b> -0.21 cm (-0.083 in)	<b>Standard deviation of the mean in X</b> 1.29 cm (0.51 in)
<b>Overall mean in Y direction</b> 1.82 cm (0.72 in)	<b>Standard deviation of the mean in Y</b> 1.62 cm (0.64 in)

The results here again show the variation in the mean offset between runs. The ensemble standard deviations depend almost entirely on the variation in the means. If the mean value of the GPS position of a single surveyed point were statistically stationary, then the ensemble standard deviation would equal the standard deviation of a single run, however, we see that this is not the case. The standard deviations of the single runs are much lower than the ensemble standard deviation at a point. The graphs also clearly show that the data for each run falls close to the mean, and it is the mean which shifts between test runs (to be discussed later).



*Absolute Accuracy of Static DGPS*

The covariance matrices were reasonably constant for the survey nails even though the tests were run on different days and at different places on the track. This means that the variance of the error of the GPS system does not change with time or position. This is in contrast with the mean offset errors of the GPS system which did exhibit some variation. Of all the tests we ran, the worst case offsets and standard deviations were seen at survey nail 63 during the second run on 11/09/95. This run had mean offsets of 5.181 cm in X and 7.779 cm in y, as well as standard deviations of 1.849 cm in X and 3.102 cm in y.

We tabulated statistics for all of the static data in an effort to determine the overall parameters of the static DGPS system. These are listed in Table 2.5 below. These values encompass data from every survey nail tested on every test run during all of the testing days (32 runs all together, taken during 3 sessions spanning 43 days).

Table 2.5 Overall Static DGPS Statistics

		<u>Overall</u>		
<b>Mean X offset</b>	<b>X std. dev.</b>	<b>Cov run 1 (cm*cm)</b>	<b>X</b>	<b>Y</b>
0.71 cm (0.28 in)	0.52 cm (0.20 in)	<b>X</b>	0.270	0.095
<b>Mean Y offset</b>	<b>Y std. dev.</b>	<b>Y</b>	0.095	0.710
1.19 cm (0.47 in)	0.83 cm (0.33 in)			
<b>Standard deviation of mean in X</b>		<b>Standard deviation of mean in Y</b>		
3.01 cm (1.19 in)		3.98 cm (1.57 in)		

The overall means in X and Y are relatively close to zero, but that is only because there were many offsets that were positive and many that were negative, as seen on the various graphs. A negative offset in Y means the GPS determined position was south of the true nail position, and a negative offset in X means the GPS determined position was west of the true position.

Based on our results, it seems that the position calculations of the GPS system did exhibit more error in the Y direction (latitude). The mean Y offset listed above is over twice as large as the mean X offset. The standard deviation in Y is also significantly larger than in X. The covariance matrix shows that the variance in the Y direction is much larger than the variance in the X direction as well. The off-diagonal terms in the covariance matrix represent the expected value of X times Y, or the covariance of X and Y. These terms are very small, suggesting that the error in the two

directions is uncoupled. At the 95% level of confidence calculated with 32 points (the number of survey nails evaluated during the static tests), the covariance value ((xy) of 0.095 (see Table 2.5) is statistically significant, but the value is so small, that it practically has no effect.

### *13 Day Continuous Log*

On December 21, 1995, we installed the DGPS antenna on top of a tripod 7 ft above the G8680 MA geodetic monument (see Figure 1.2 for location) and collected data for 13 consecutive days. The computer and GPS receiver were housed in a heated cabinet near the monument. A 5 ft tall chain link fence which ran approximately 4 ft from the tripod and a 5 ft tall metal cabinet located 10 ft from the tripod were the only objects near the antenna. Data was collected at 5 minute intervals for the purpose of determining whether any long term trends existed in the position solution of the DGPS system.

Upon analysis, we found the following statistics: 3.37 cm mean offset in the Y direction and 7.61 cm mean offset in the X direction (see Figures 2.21, 2.22 and 2.23). Clearly, there was an oscillatory pattern in the data and therefore it was not meaningful to compute a standard deviation from the overall mean. The oscillation had an average amplitude of 5.19 cm in X and 4.62 cm in Y, and an average period of 12 hours at the 95% level of confidence. This oscillation may explain the drifts in the offsets seen earlier in our previous data. Also, the data shows that there was an unexplained disturbance on the 9th day which lasted about 10 minutes.

We believe that the oscillatory pattern is the result of the 12 hour satellite orbits. Errors inherent in the DGPS system (such as multipath, etc...) depend on the positions of the satellites in the sky. The satellites orbit the earth every 12 hours [23], thus generating the oscillatory curve observed in Figure 2.21 (Figures 2.22 and 2.23 are magnified versions of Figure 2.21). If the oscillation is deterministic, it should be possible to compensate for it and thus improve the accuracy of the DGPS system.

In an attempt to characterize the oscillatory behavior, we plotted cycles of oscillation on top of one another in each of the X and Y directions in the hopes of finding a clear sinusoidal trend. We found that almost no trend could be seen in the Y direction because the data was too noisy to discern a pattern. In the X direction a definite oscillation could be distinguished, but this too was quite noisy. Not only was it noisy, but it varied quite drastically in amplitude, so much so that we could not fit a curve to it with greater than a 60% level of confidence. Graphs of the variation in the amplitude of X, best and worst case, are shown in Figures 2.24 and 2.25. Running 1 hour standard deviations were calculated for both data sets. The largest running standard deviation for

the data shown in Figure 2.24 was 2.4 cm, while it was only 1.5 cm for 28b. No graph is presented for Y since the noise was large and thus made it difficult to distinguish a significant trend. (There is a slight oscillatory pattern present.)

Figure 2.24 shows that the amplitude of the oscillation in the X direction can vary by over 5 cm. The high degree of variability of the oscillatory pattern in both the X and Y directions makes it difficult to accurately model the oscillation at this point. The source of daily variation may be due to multipath effects at the base station. Another effect which may cause biases or noise in the results is the residual effect of ionospheric distortions not completely removed by the differential correction. Further research may clarify the issue.

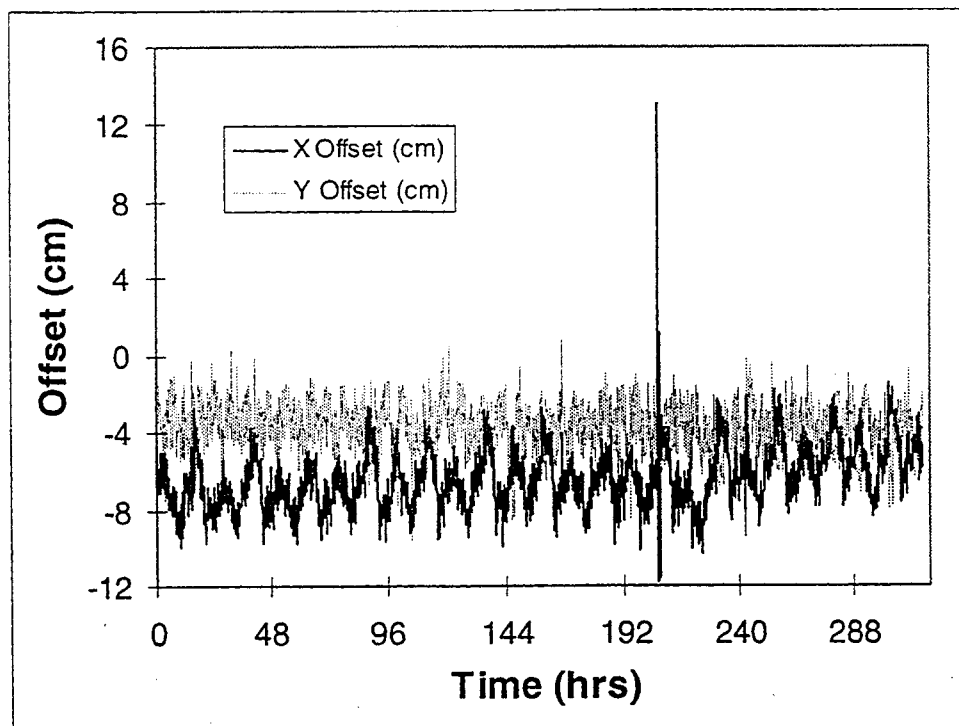


Figure 2.21 13 day continuous DGPS log at monument: position offset from true. Data collected at 5 min intervals.

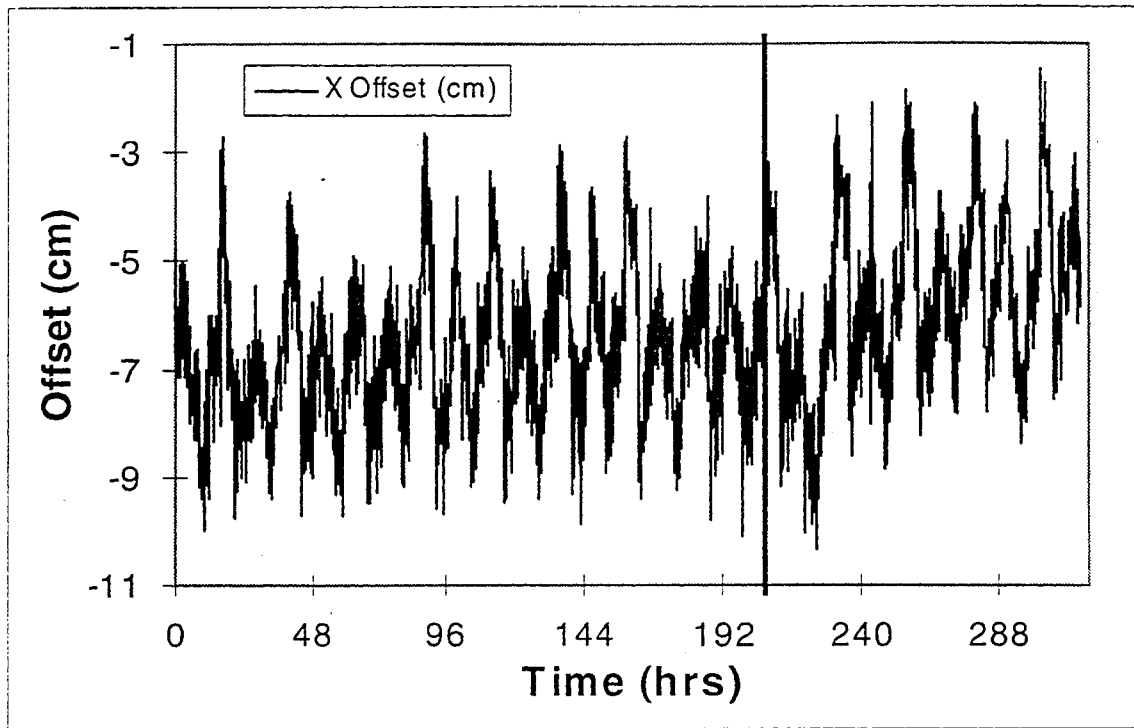


Figure 2.22 Close-up of X offset during 13 day continuous DGPS log at monument. Data collected at 5 min intervals.

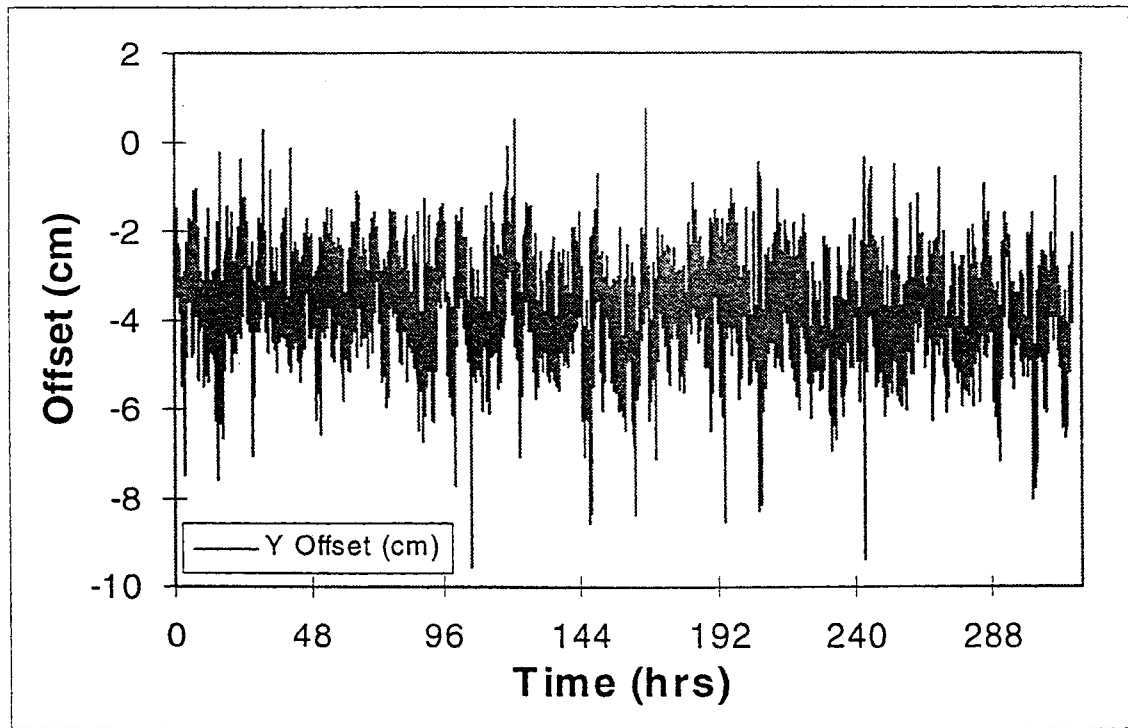


Figure 2.23 Close-up of Y offset during 13 day continuous DGPS log at monument. Data collected at 5 min intervals.

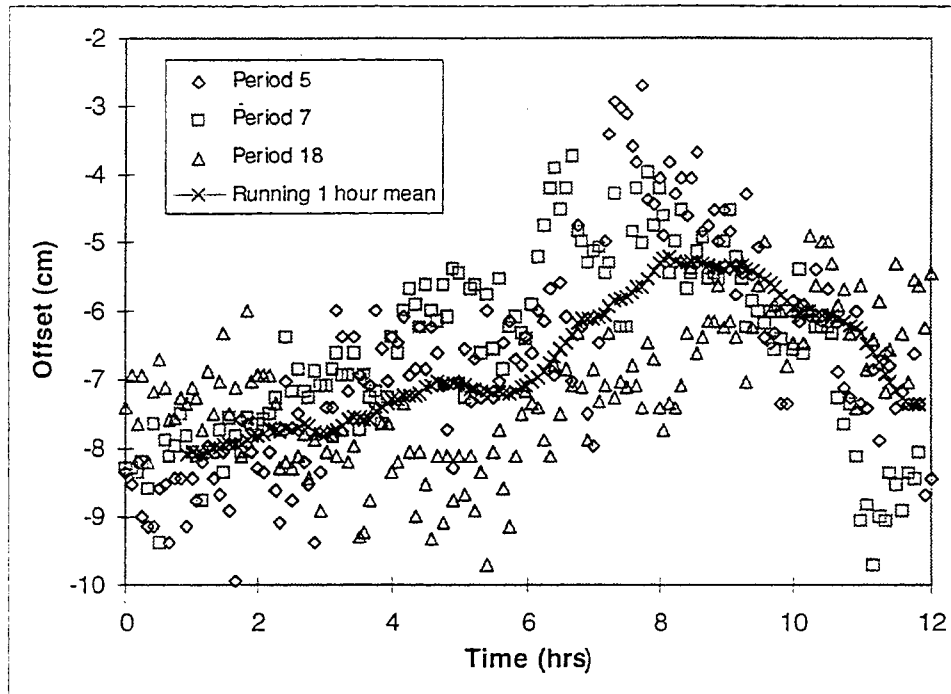


Figure 2.24 Variation in X over three periods of oscillation in the DGPS system: most variation. Time at 0 corresponds to 3 am and 3 pm.

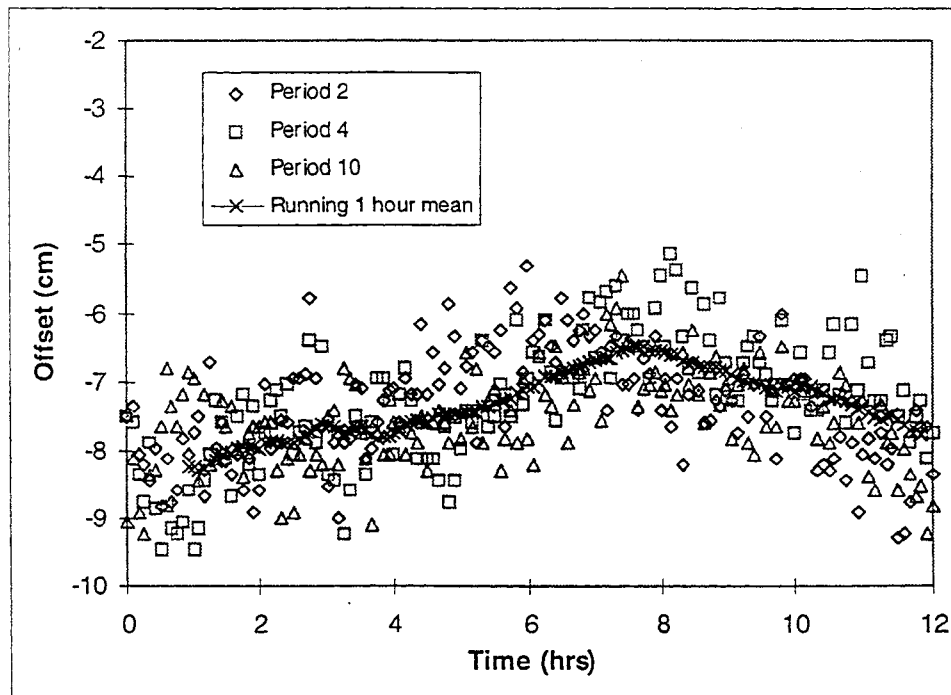


Figure 2.25 Variation in X over three periods of oscillation in the DGPS system: least variation. Time at 0 corresponds to 3 am and 3 pm.

### *Relative Accuracy of Static DGPS*

#### *Long Distance Measurements*

We calculated the distance between the DGPS determined positions of twenty-one pairs of survey nails taken during different times on three different occasions, all during the mid afternoon. The purpose of this test was to determine how the GPS system performed in measuring distance in the relative sense, as opposed to the tests described previously which were measures of absolute accuracy. These tests quantify how well distance can be measured by comparing one GPS derived measurement to another. Relative accuracy is of particular interest because of the nature of our application. We plan to use the DGPS to develop a digital "map" of each of the lanes of the Mn/ROAD track. This "map" would be made by finding the mean path of multiple laps made around each lane (see Section 3.2.5). One determination of whether a vehicle is under acceptable driver control (due to fatigue, for example) would be made by monitoring the vehicle's lateral position and yaw with respect to the digital "map." In the future, such a digital "map" could be available on a CD-ROM or equivalent, and would essentially be an additional layer (containing number and location of lanes, locations and widths of shoulders, etc...) residing on existing GIS road data bases.

Upon comparing the DGPS determined distances to the surveyed distances, we found: The GPS system calculated distances of 122 m (400 ft) to 700 m (2300 ft) with a mean error of -2.3 cm (0.9 in) and a standard deviation of 3.3 cm (1.3 in) (see Figures 2.26 and 2.27). The error did not seem to be a function of the distances measured. Note that some of the error in these results may be due to the oscillatory behavior in the DGPS readings discussed earlier.

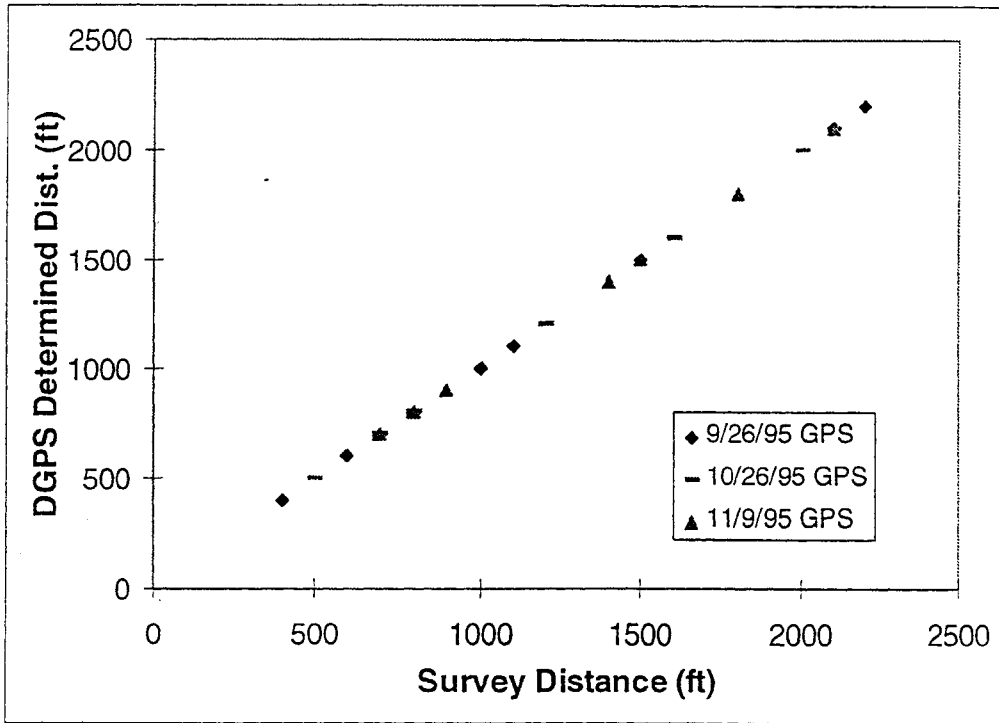


Figure 2.26 DGPS long distance measurements during 3 test sessions

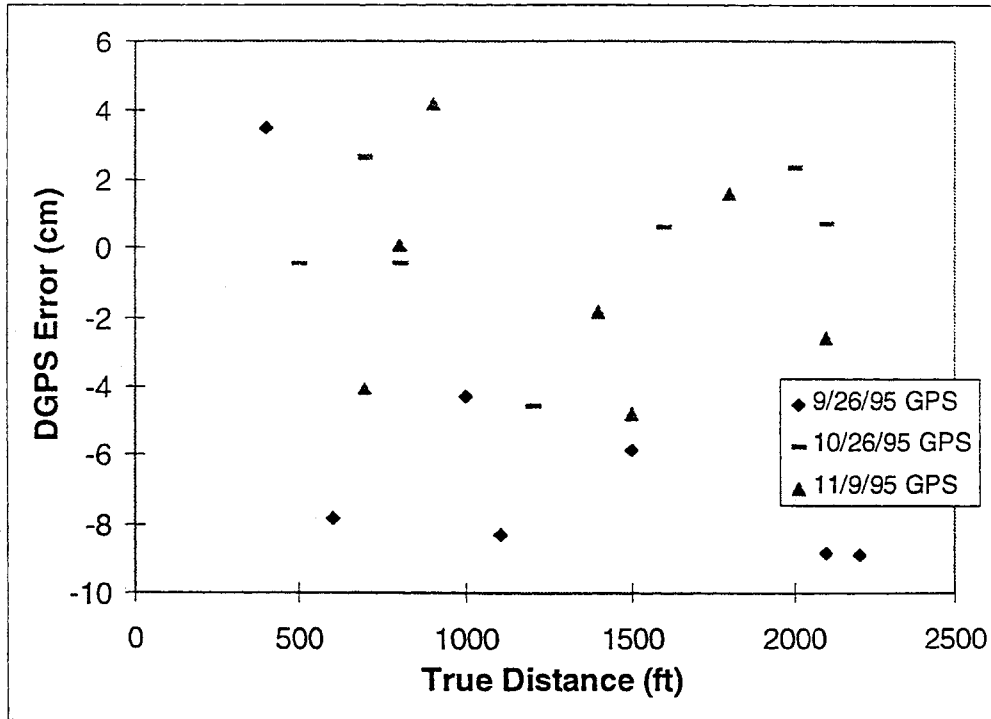


Figure 2.27 DGPS error in long distance measurements during 3 test sessions

### *Short Distance Measurements*

The following shows that the GPS system also performs well at short distances. Given the nature of our objectives, i.e. to measure the truck's lateral offset from the lane's center, we are interested in how well the system performs over short distances.

For this test, we laid down a tape measure on the road and measured out a number of distances ranging from 0.6 to 18.3 m (2 to 60 ft). We then moved the GPS antenna along the tape measure and recorded the positions. This test was run on three different occasions, all during the late afternoon. Upon comparing the DGPS determined distances with the measured distances, we found the system to have a mean offset of 1.26 cm (0.49 in) and a standard deviation of 2 cm (0.8 in) (see Figures 2.28 and 2.29). Note again that some of the error in these results may be due to the oscillatory behavior of the DGPS readings discussed earlier.



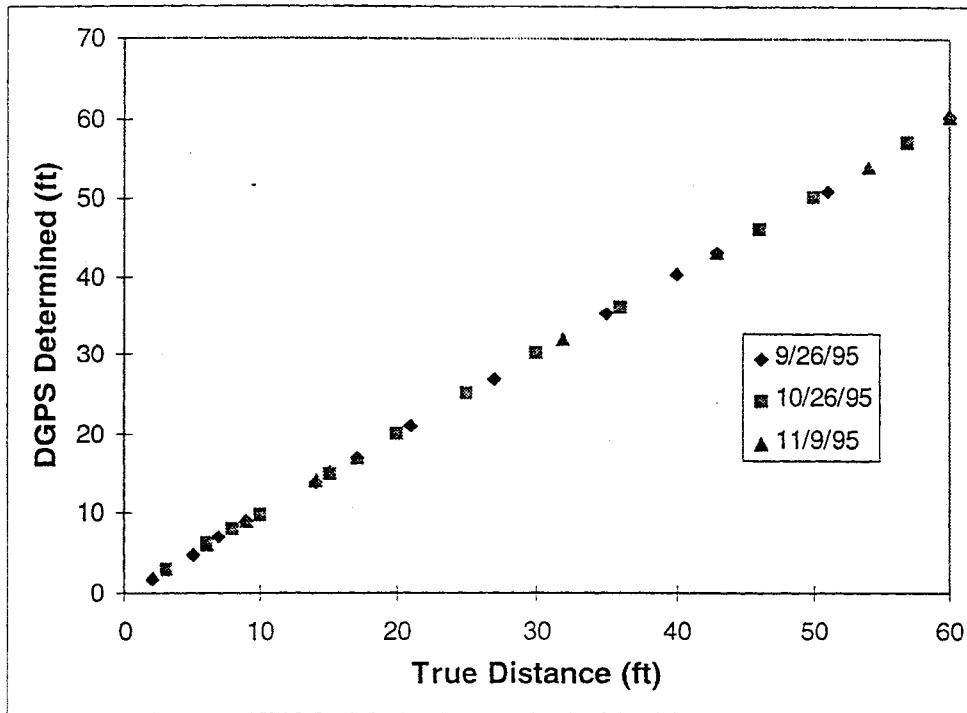


Figure 2.28 DGPS short distance measurements during 3 test sessions

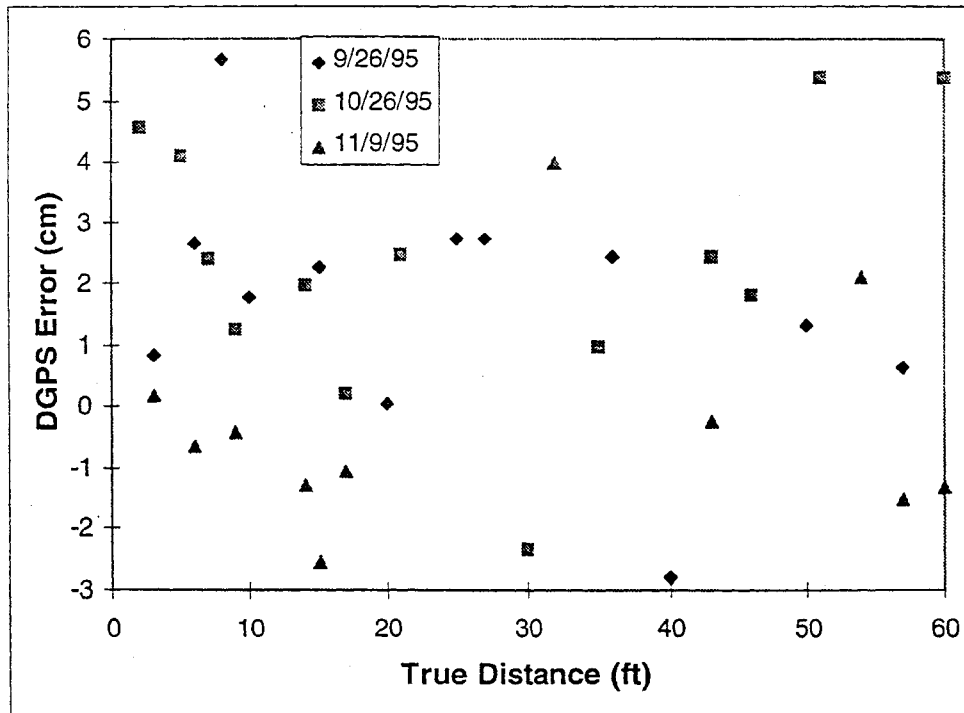


Figure 2.29 DGPS error in short distance measurements during 3 test sessions

### *Effect of Blocking Antenna*

The DGPS system relies on the position signals of numerous satellites to compute its own position. Therefore, if an obstacle blocks the antenna from receiving satellite signals, the position solution will degrade. If enough satellites are blocked, then the solution will be lost all together and the system will have to start recalculating a new solution. This is referred to as “loss of lock” from which it may take up to an hour to fully recover.

To calculate the effect of such blockage, we partially and fully covered the GPS antenna while the system was collecting data at a survey nail (see Figures 2.30 - 2.32). We found that partial blockage had an insignificant effect on the solution so long as 4 or more satellites were still in view (see section of Figure 2.32 from 60 to 80 seconds). However, if fewer than 4 satellites were available, then the system lost lock. Upon regaining lock, the system calculated positions with accuracies on the order of 20 cm, but took up to an hour for the system to reconverge to a solution whose accuracy was within a few centimeters. In this example, it took approximately 200 sec (3.3 min) for the mean offset in Y to come within 20 cm, but it took 9 minutes for the offset in X to reach 20 cm. It is for this reason that we feel that is imperative that the GPS signals be combined with an inertial measurement system until newer, more robust, GPS systems become available (for example, new dual frequency units).

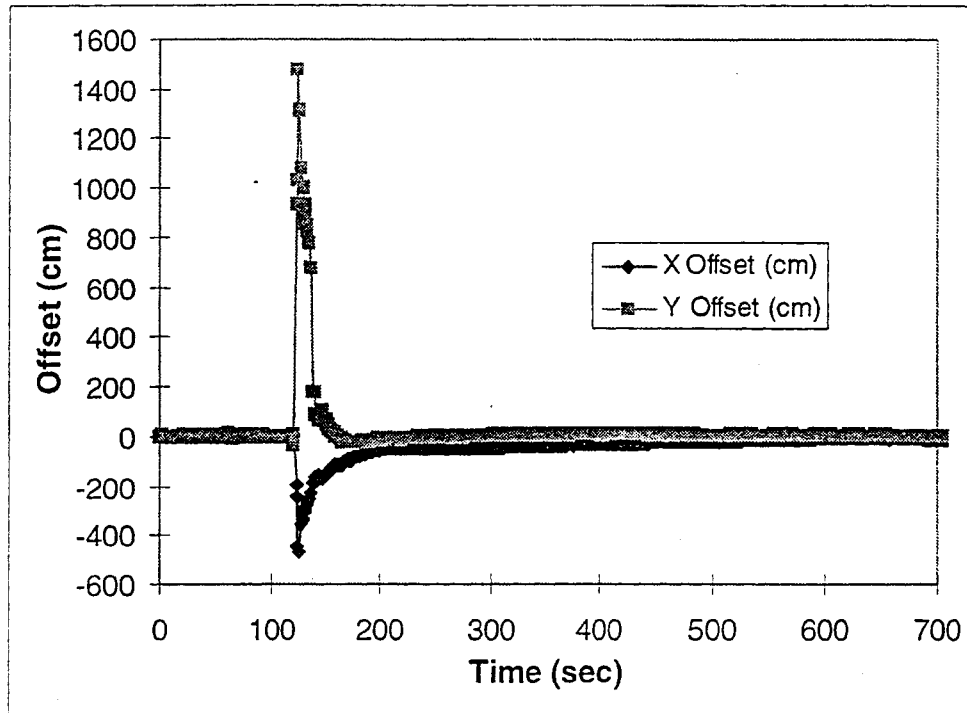


Figure 2.30 11/09/95 Static DGPS convergence, recovery following full cover at survey nail 101

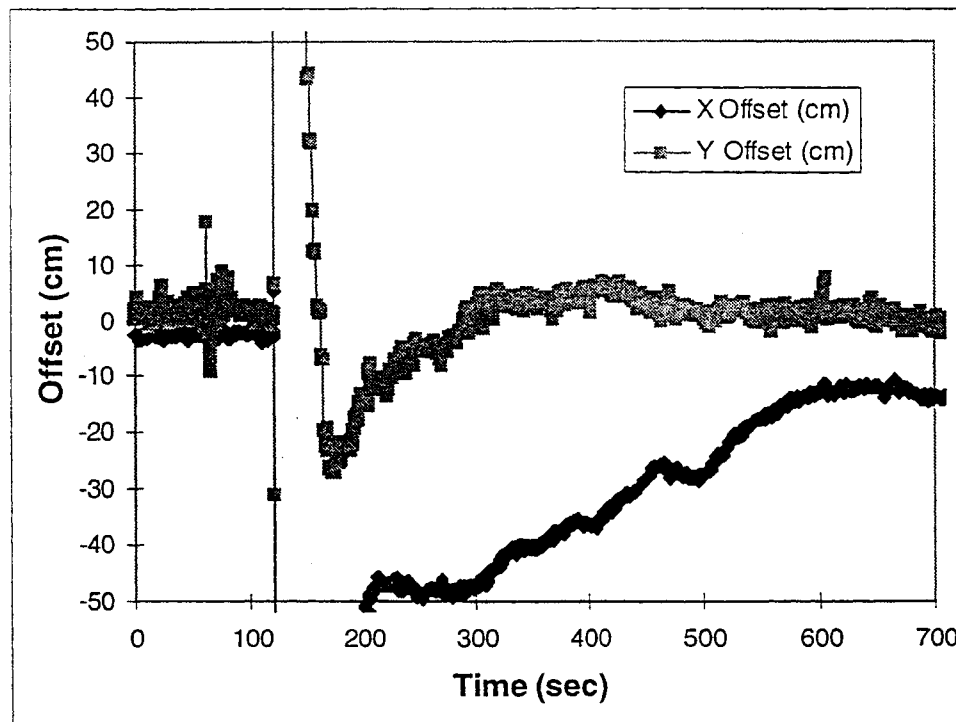


Figure 2.31 11/09/95 Close-up of static DGPS convergence, recovery following full cover at survey nail 101

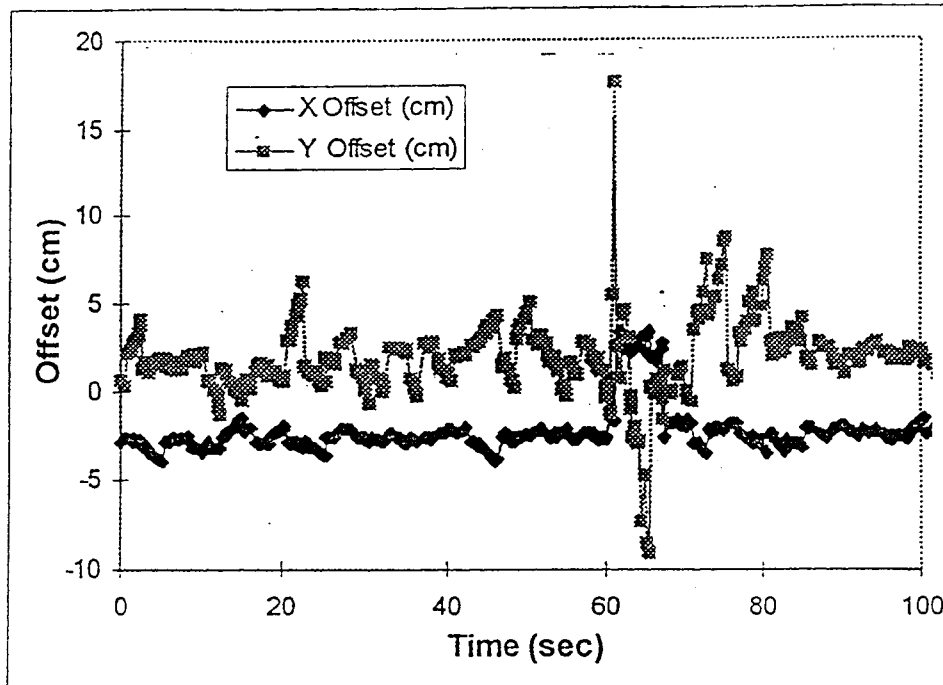


Figure 2.32 11/09/95 Static DGPS convergence, recovery following partial cover at survey nail 101 (beginning at 60 sec)

Bridges do present a serious obstacle to using GPS alone for vehicle guidance unless changes are made to the algorithms which compute GPS location. If the GPS technology does not change, then one approach might involve combining the results from two GPS antennas located on opposite ends of the tractor-trailer unit.

We found that the most reliable indicator of loss of lock was the “RT20 Position Status” flag (RT20 status) in the position log provided by the GPS. To test the reliability of this flag, we collected DGPS position data while we drove the truck on a 31-mile stretch of I-94, passing under 11 bridges. Upon analyzing the data, we found that the GPS system lost lock under every bridge because no satellites were visible to the GPS antenna. We also found that the RT20 status correctly indicated when loss of lock had occurred.

While the RT20 status flag seems to be a reliable way of determining loss of lock, it is not enough for vehicle guidance purposes. The RT20 status does not indicate anything about the accuracy of the solution, only that a solution is being calculated. The flag will read “Good Solution” as long as the GPS system is operating correctly (i.e. within the vendor’s

specifications), regardless of how accurately the solution has converged. Therefore, the GPS position errors may be greater than tolerable for keeping the vehicle in its lane, but the RT20 status would not indicate that something was wrong. These considerations further emphasize the need to augment the GPS system with an inertial measurement system.



## CHAPTER 3

### Evaluation of Dynamic Performance

#### *Description of Experiment*

This set of experiments determined the position accuracy and repeatability of the NovAtel DGPS system while the GPS receiver antenna was mounted on the Navistar truck and traveling between 20 and 35 miles per hour.

For the dynamic experiments, we aligned a CCD (charge-coupled device) camera directly below the GPS receiver antenna and mounted them as a unit two feet off to the side of the truck, as shown in Figure 3.1. The camera/lens array was mounted to be concentric with the GPS receiver antenna. The camera's field of view at 9 ft above the ground was 4 ft. by 3.7 ft. The image pixel array size was 640 H x 486 V. To avoid blur during motion, the camera was operated at a shutter speed of 1/2000 sec. A computer-controlled VCR (JVC #BR-S822DXU) with very accurate time/speed controls recorded the images from the camera and encoded each frame with a time-stamp [21]. The real time accuracy of this VCR was specified to be no worse than 1.8 seconds per hour (0.05%). During a run, the computer recorded a time-stamp for each GPS position as it was received in order to correlate the ground position with the GPS position reading. Square ceramic tiles (measuring 29.8 cm + 0.1 cm per side) were mounted on the ground at each survey nail. The tiles were aligned along the north axis with one corner centered at the survey nail itself (see Figures 3.2 and 3.3). These were used in order to (1) ensure that the survey nail position was visible to the camera, (2) to monitor whether the camera was aligned perpendicular to the road, (3) to verify that there was no distortion in the lens and (4) to determine the yaw angle of the vehicle with respect to north. The yaw angle was used to convert from the absolute reference frame aligned with the north and east axes to the instantaneous vehicle reference frame aligned in the direction of motion and perpendicular to vehicle motion. We also measured the distance between the survey nail and the GPS receiver antenna position at the time the GPS log was received in terms of the camera coordinates (dx and dy) in order to be able to correct for this offset.

During the experiments, we drove the truck around the track so that the GPS receiver antenna and camera passed above the survey nails and tiles. The VCR recorded images at 30 Hz and the computer recorded (at a temporal resolution of 1/100th of a second), GPS position logs and VCR time-stamps at 5 Hz. Data was collected while driving numerous laps (8 and 11, respectively) around the track during the mid afternoon on two separate days. Dynamic DGPS accuracy was analyzed at a total of 48 survey nail locations. Data collection began once the DGPS system had converged (typically 1 hour after satellite lock). Our data acquisition system waited for the GPS to

send it a position log, and, upon receiving the log, acquired the corresponding time-stamp for the current frame on the VCR (see Figure 3.4). This ensured that there was an image of the ground corresponding to each position that was recorded from the GPS. The code used to interface the DGPS system with the time-stamp VCR and to collect data is documented in Appendix B.

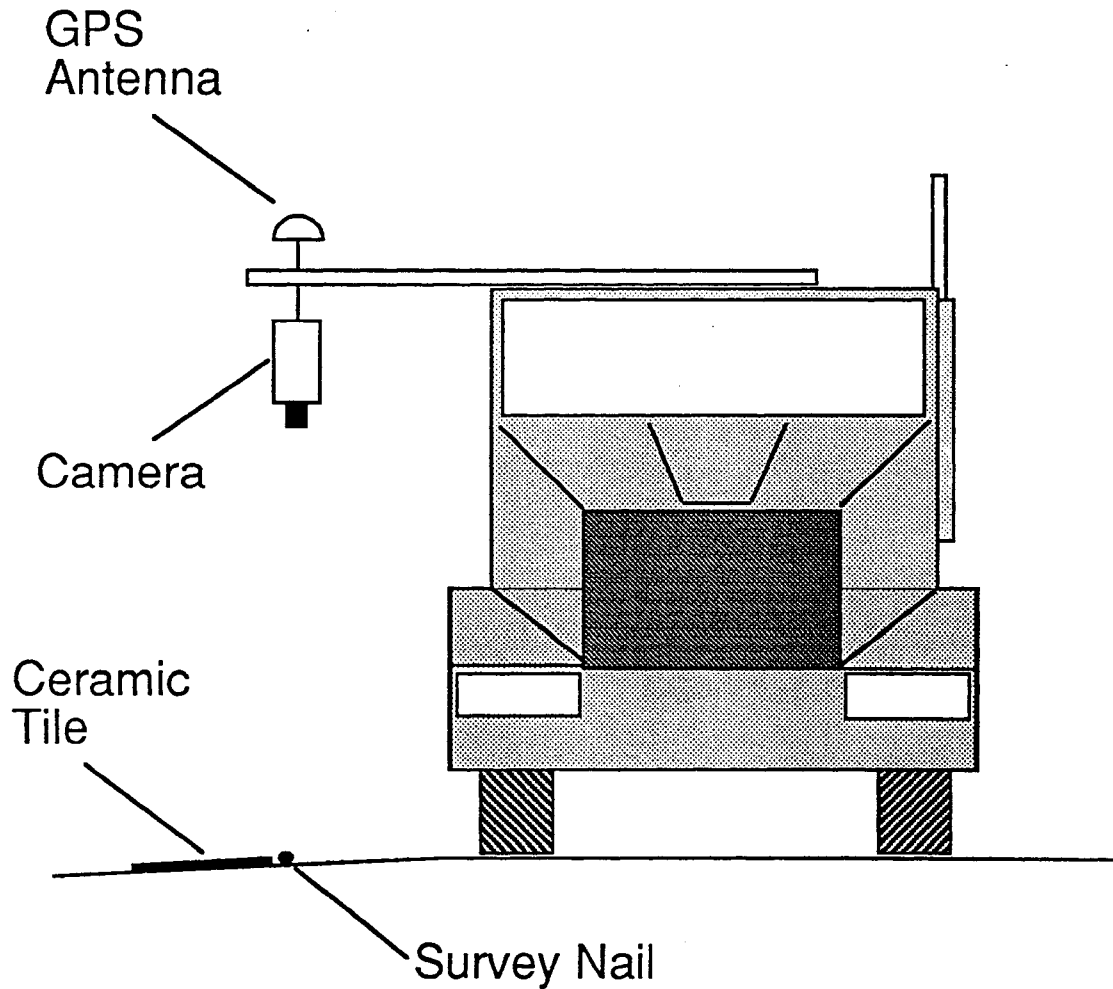


Figure 3.1 Dynamic DGPS accuracy experimental configuration (Not to scale.)



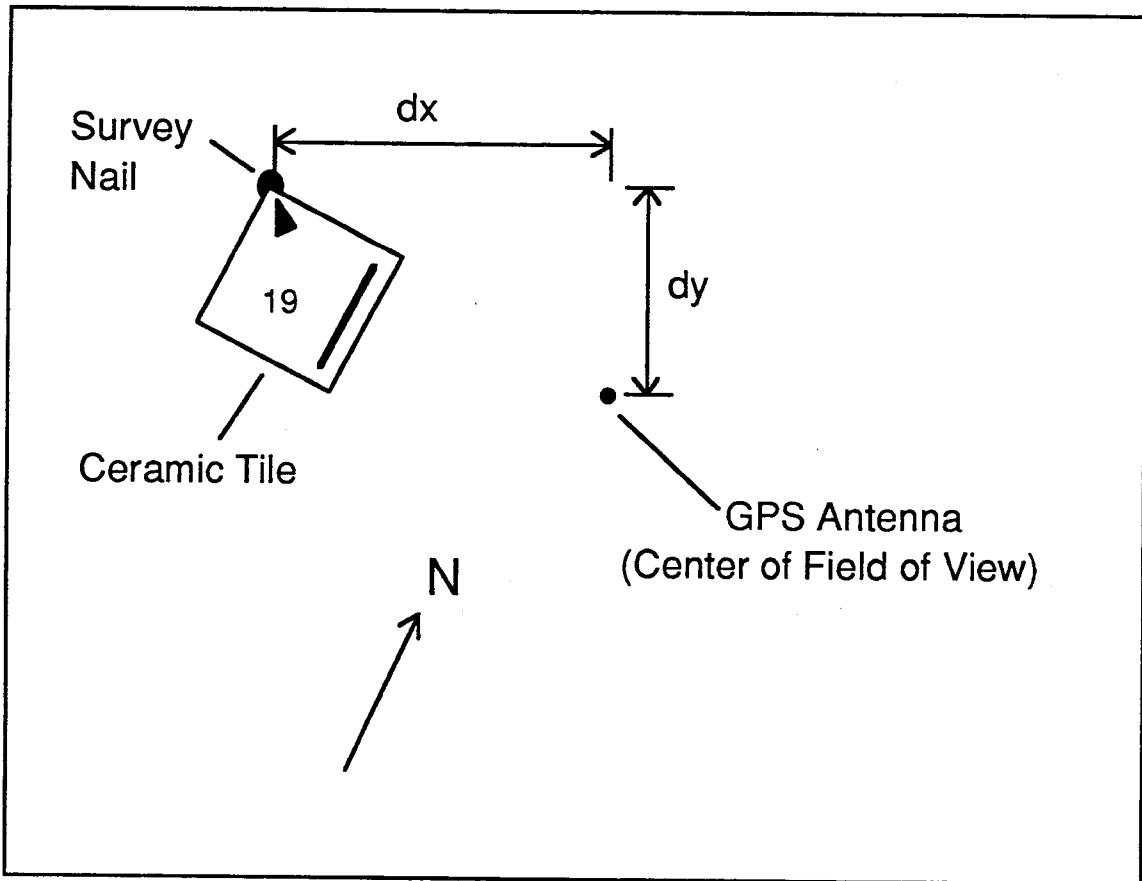


Figure 3.2 Camera field of view showing correction for GPS antenna position (line on tile indicates north)



Figure 3.3 Image of tile and survey nail as seen by camera. (Note arrow pointing at survey nail and line on edge indicating north. Light areas on top and bottom are snow.)

To analyze the dynamic DGPS accuracy at each survey nail location, we needed to calculate the distances between the GPS receiver antenna and the survey nail along the north and east directions. To do this, we used a frame grabber board (Indigo 2 Video Board, Silicon Graphics Inc., 640 V x 486 H) to capture the images from the videotape. Once the images were captured, we digitized points in the image including the position of the GPS antenna (center of the field of view), the center of the survey nail, and the corners of the tile. These points were used to calculate the offsets in north and east coordinates. We also checked the four corners of the tile to ensure that the image of the tile was exactly square. A perfectly square tile in the image indicated that the camera was perpendicular to the ground when the image was taken. If the camera was oriented at an angle off the vertical, then the tile would appear as a trapezoid. This test was important to ensure that there was no distortion in the offset distances measured from the image. This code is documented in Appendix C. Note that the fiducial points were digitized by hand, where an error of a few pixels in each measurement may be possible. This inaccuracy should be taken into account in evaluating our results.

Given the lens, the focal length and the distance of the field of view from the imaging array, each pixel represented an area measuring 0.23 cm (v) x 0.19 cm (h). At this resolution, it was not possible to perceive any pincushion or trapezoidal distortion in the tile.

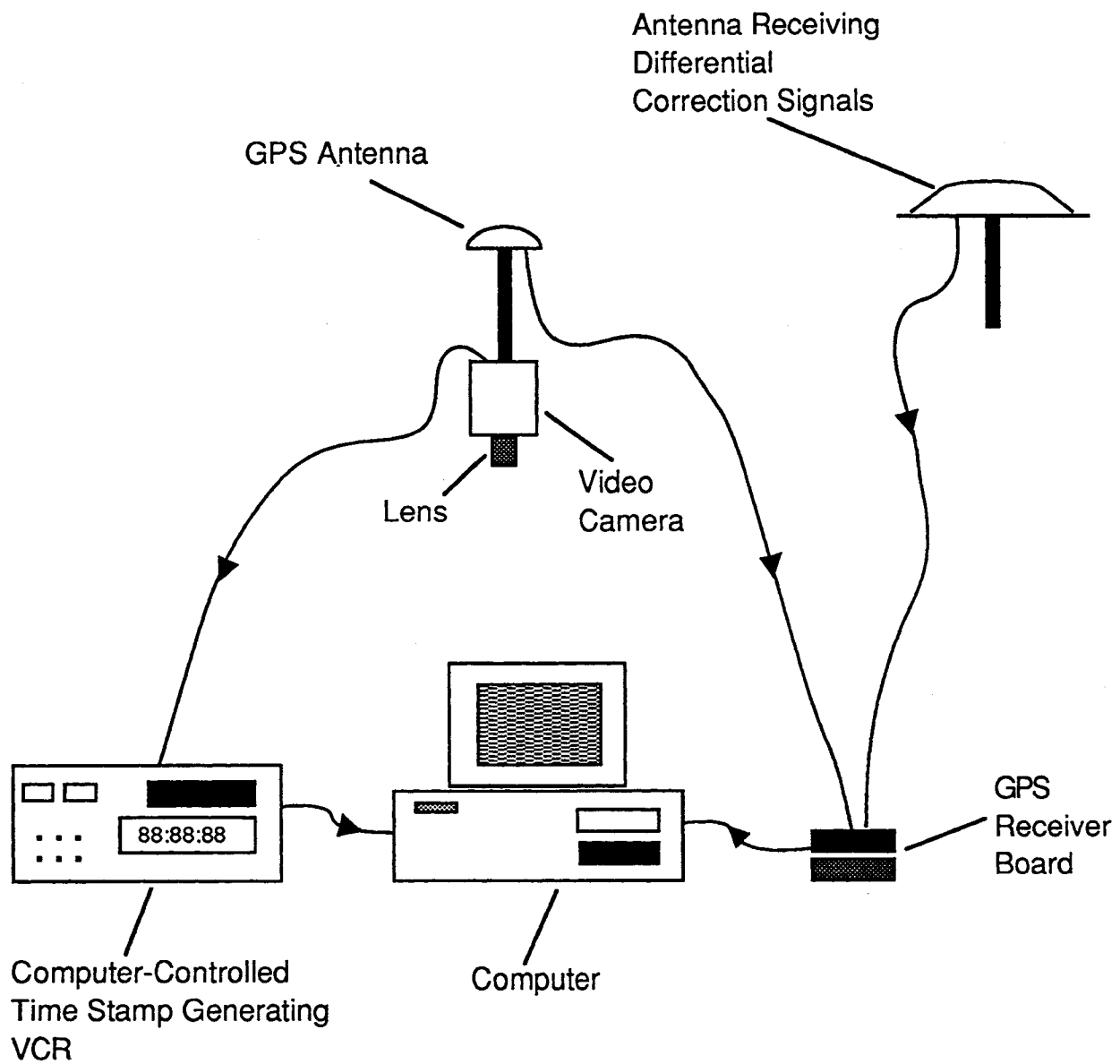


Figure 3.4 Data acquisition for dynamic DGPS evaluation

## *Results*

The results of the dynamic tests were broken down into two components: error in the direction of vehicle motion and error perpendicular to the direction of vehicle motion. While the static results were analyzed in terms of X and Y (longitude and latitude), it was not meaningful to analyze the dynamic results in this way. For the purpose of vehicle tracking and guidance, errors in the direction of motion and perpendicular to motion are the important parameters since the vehicle constantly changes its orientation with respect to an absolute reference frame (see Figures 3.5 and 41). Note that in the direction of motion, a positive error corresponds to a GPS position located behind the vehicle's actual antenna location, while a positive error perpendicular to the direction of motion corresponds to a GPS reading to the right of the vehicle's actual antenna location.

To determine the error in the direction of motion (DM) and perpendicular to the direction of motion (PDM), we analyzed the images of the survey nails taken by the camera. As the truck drove over a survey nail and tile, the camera recorded images at 30 Hz. On the video tape, the survey nail appeared on 3 to 4 consecutive frames, moving across the screen from frame to frame. We determined the "instantaneous" velocity vector, indicating the direction of vehicle motion as it went over each survey nail by digitizing the location of the survey nail and tile in the consecutive frames. Using the tile orientation, we computed the vehicle's yaw angle with respect to north. We then defined a vehicle coordinate frame with axes along the direction of vehicle motion (vehicle longitudinal axis) and perpendicular to vehicle motion (vehicle lateral axis). The errors that had been calculated in X and Y (based on the surveyed locations of the nails) were converted into the new coordinates. To do this we used the code documented in Appendix C.

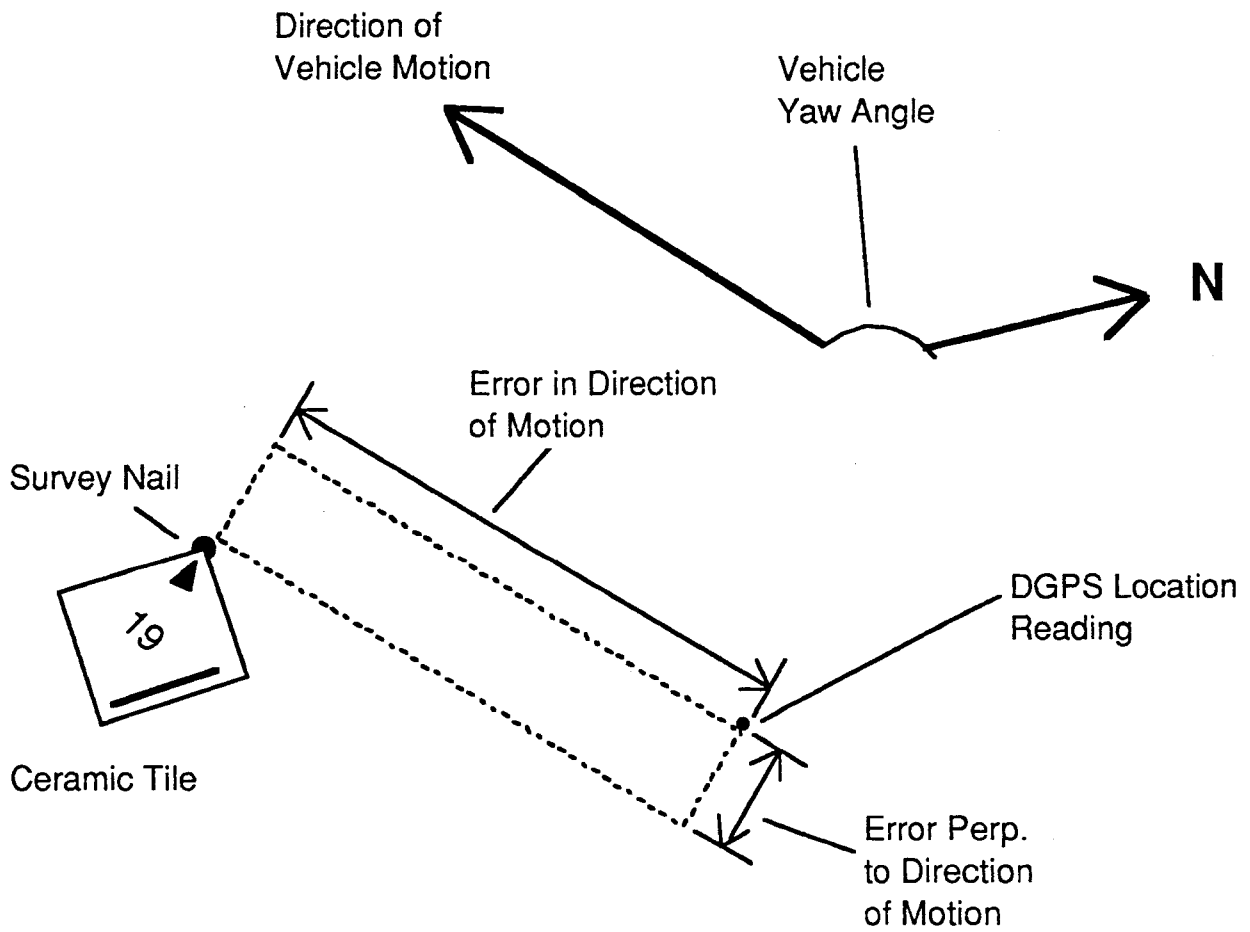


Figure 3.5 Dynamic error in direction of motion and perpendicular to direction of motion

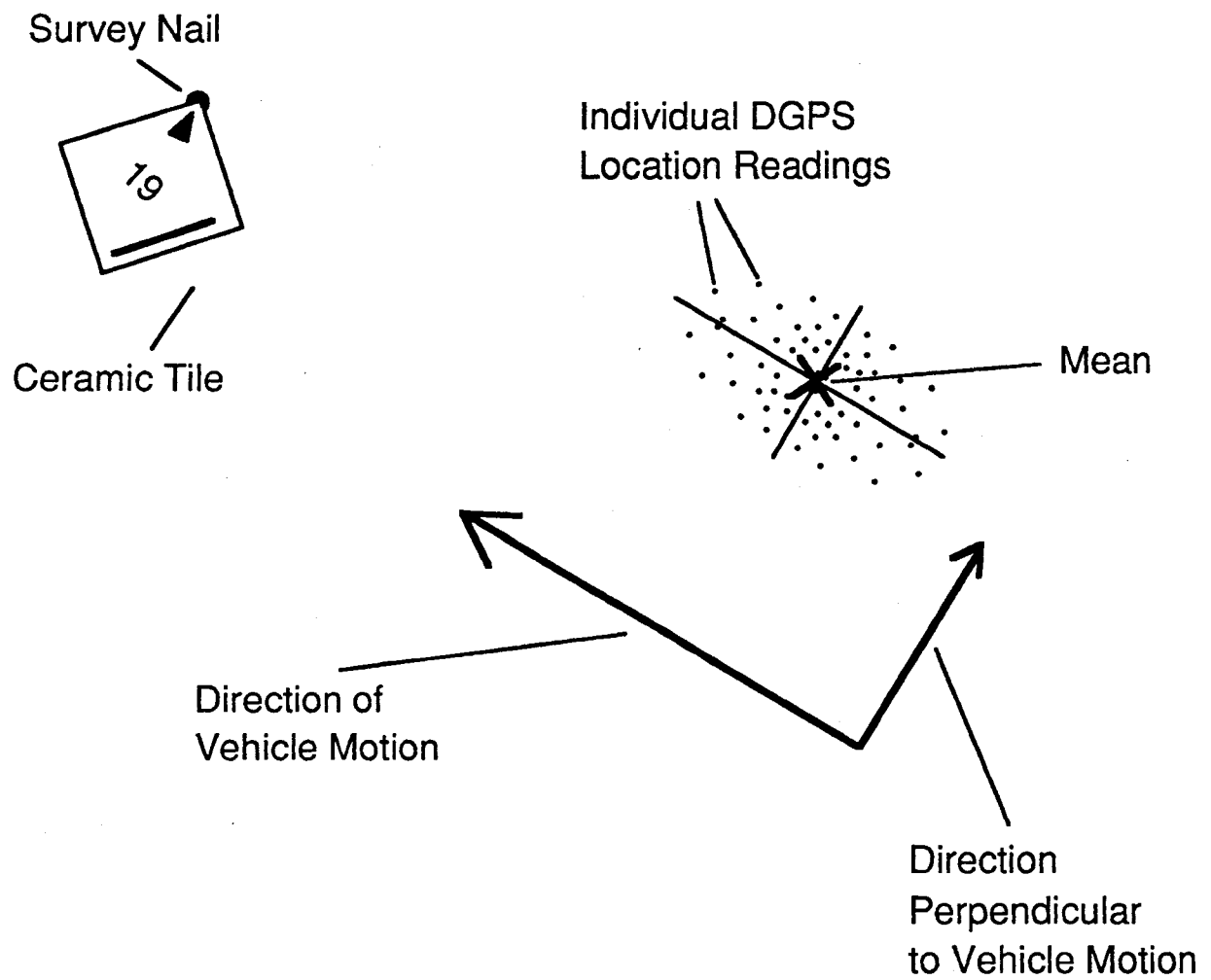


Figure 3.6 Dynamic error in direction of motion and perpendicular to direction of motion: variance of data

There is a specified 70 ms latency associated with the data generated by the NovAtel GPS system. This means that the position which the GPS system generates corresponds to the position where the GPS antenna was located 70 ms earlier. In addition, it takes approximately 10 ms for our data acquisition system to acquire the position from the GPS receiver. Thus, there is an effective 80 ms latency in the system, which does not present a problem for the static tests, yet has significant implications for the dynamic tests. These latencies are illustrated in Figure 3.7. Since the GPS antenna is moving, the position readings that are received do not correspond to the current position of the GPS antenna, but rather to its position some distance back. Given the nature of the latency, this distance error will change with speed. At 20 mph, 80 ms latency would result in 0.716 m (2.35 ft) of error in distance along the direction of motion. At 35 mph, the latency would result in 1.25 m (4.10 ft) of error. Since the system latency should only affect the accuracy of the position in the direction of motion, separating the analysis into the two components should allow us to investigate the error due to the latency and thus to better characterize the actual GPS error as a function of vehicle velocity. Furthermore, if our hypothesis is correct, this approach provides us with a means for correcting for latency by using auxiliary sensors that provide us with an independent measure of the instantaneous velocity vector (e.g. as would be derived from vehicle mounted longitudinal and lateral accelerometers).



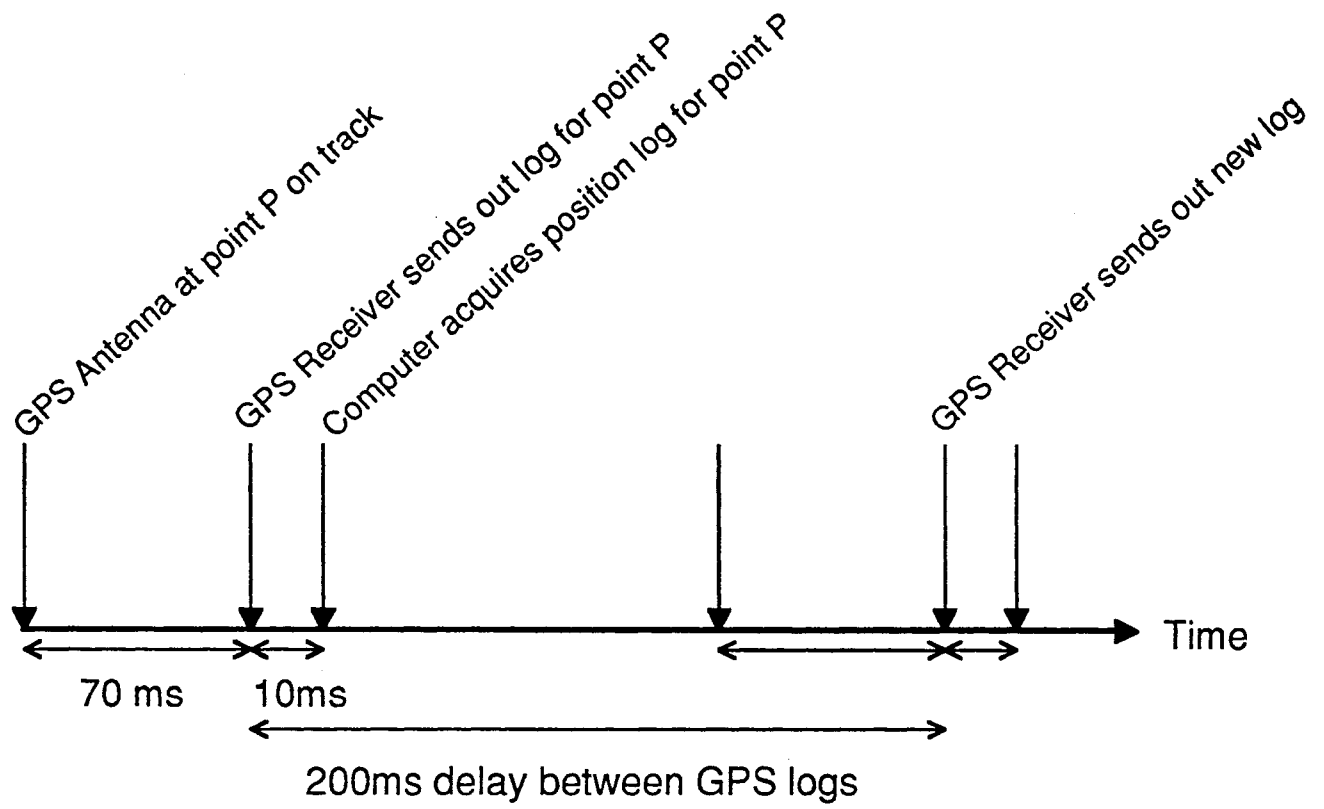


Figure 3.7 Timing diagram of dynamic DGPS data acquisition

To account for the 80 ms latency, we calculated the distance error due to latency for the “instantaneous” velocity of the truck at each survey nail and subtracted these distances from the error measured in the direction of motion at each survey nail. Through this process we attempted to isolate the residual error inherent in the DGPS system, which is independent of the GPS latency. Our data consisted of 9 survey nails on the straight road sections (speeds from 29 to 35 mph) and 39 on the curves (speeds from 20 to 29 mph). All of the data presented is statistically significant at the 95% level of confidence.

*Error in the Direction of Motion*

Figure 3.8 shows the dynamic DGPS error in the direction of motion for all of the survey nails. This figure shows the raw values, before adjusting for the latency in the system. Figure 3.9 shows the same data adjusted for the latency at each survey nail. The error decreased dramatically with the latency based correction. The results are summarized in Table 3.1 below.

Table 3.1 DGPS Error in the Direction of Motion

<u>Straight section (29 to 35 mph)</u>		
	<u>Raw</u>	<u>Latency Adjusted</u>
Mean offset	91.43 cm (36 in)	-21.7 cm (-8.54 in)
Std. dev.	28.87 cm (11.37 in)	29.31 cm (11.54)
<u>Curved road section (20 to 29 mph)</u>		
	<u>Raw</u>	<u>Latency Adjusted</u>
Mean offset	76.84 cm (30.25 in)	-15.35 cm (-6.04 in)
Std. dev.	28.36 cm (11.16 in)	27.42 cm (10.79)
<u>All Nails</u>		
	<u>Raw</u>	<u>Latency Adjusted</u>
Mean offset	78.70 cm (30.98 in)	-17.34 cm (-6.83 in)
Std. dev.	26.76 cm (10.53 in)	25.54 cm (10.06)

The error of the system on the curves is almost identical to the error on the straight section in both mean and standard deviation. We believe that the shift of the mean offset from a large positive number to a smaller negative number is because our estimate of the 80 msec latency was (a) too large and (b) not necessarily constant. Note that there is quite a bit of variation among the DGPS readings at each survey nail. We believe that a portion of this variation may be due to the vibration of the vehicle as it was moving.

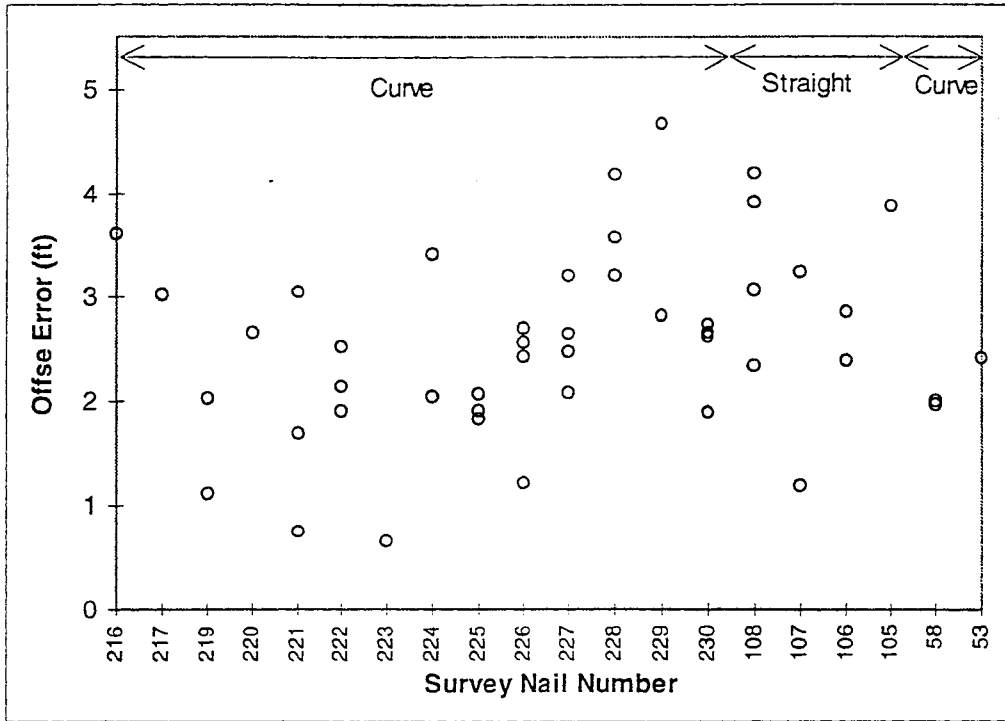


Figure 3.8 Raw DGPS dynamic error in the direction of motion at all survey nails: 3/1/96 and 3/5/96 (No data at nails 218 and 57-54)

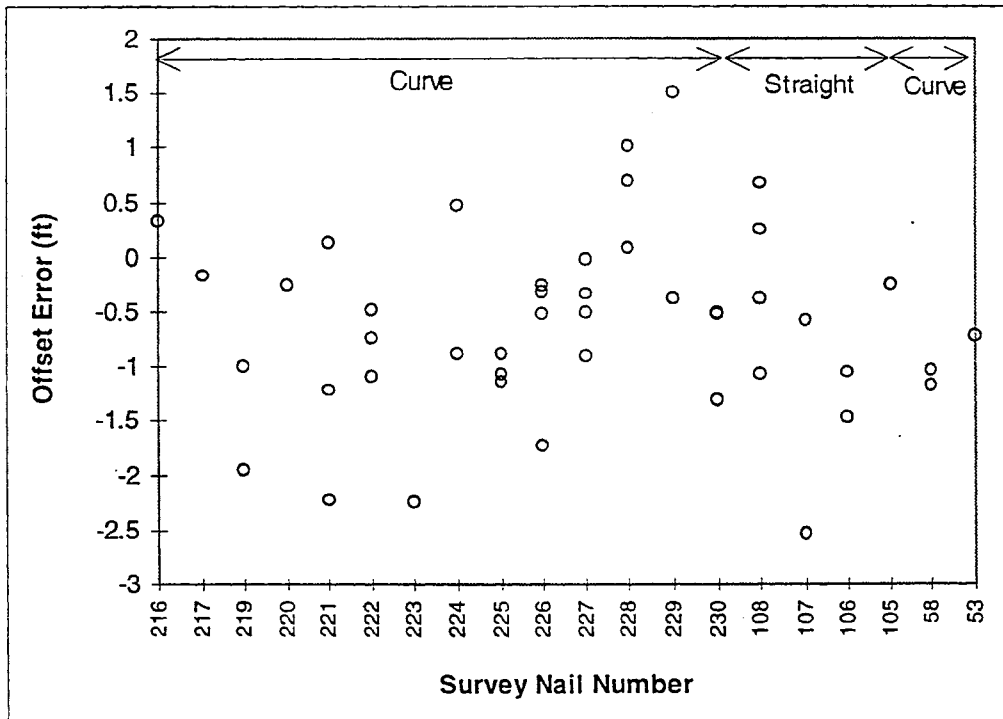


Figure 3.9 Latency adjusted DGPS dynamic error in the direction of motion at all nails: 3/1/96 and 3/5/96 (No data at nails 218 and 57-54)

*Error Perpendicular to the Direction of Motion*

Figure 3.10 shows the dynamic DGPS error perpendicular to the direction of motion for all of the survey nails. Here of course, there was no need to adjust for latency since that only affected the error in the direction of motion. The results are summarized in Table 3.2 below.

Table 3.2 DGPS Error Perpendicular to the Direction of Motion

	<u>Straight section</u>	<u>Curved road sections</u>	<u>All Nails</u>
Mean offset	2.82 cm (1.11 in)	4.97 cm (1.96 in)	4.58 cm (1.8 in)
Std. dev.	69.03 cm (27.18 in)	30.77 cm (12.11 in)	39.57 cm (15.58)

These results compare quite closely with the error in the direction of motion, leading us to believe that we have successfully accounted for the system latency. Note that the mean offsets were remarkably small but there was quite a bit of variance among the DGPS readings at each survey nail. The variation may be due in part to small angles of vehicle roll which we were unable to account for, as described above. This roll angle due to the banking of the road will have a larger effect on the error in the direction perpendicular to vehicle motion than on the error in the direction of motion. In order to determine the effect of roll, a rate gyro measuring vehicle roll ought to be included in future experiments.

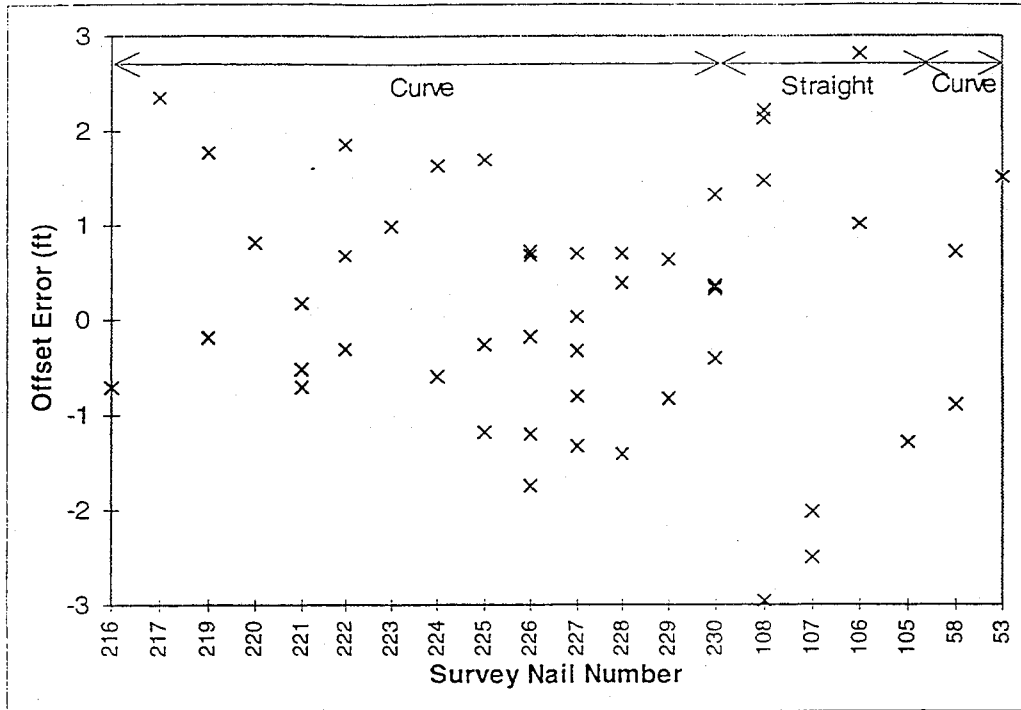


Figure 3.10 DGPS dynamic error perp. to the direction of motion for all survey nails: 3/1/96 and 3/5/96 (Note: no data at nails 218 and 57-54)

*DGPS Error Covariance*

In order to use DGPS as a sensor for vehicle guidance, we also require that the covariance of the error in DM and PDM remain small and constant. At the time that this report was prepared, we did not have sufficient data to be able to calculate covariance matrices at the 95% level of confidence for each survey nail as we had done for the static analysis. Instead, we calculated the covariance matrix of the offsets for all the survey nails we analyzed. Table 3.3 summarizes the covariance of the latency adjusted error in DM with the error in PDM:

Table 3.3 Dynamic DGPS Covariance

Cov:	<u>Overall covariance matrix (cm*cm)</u>	
	Adjusted DM	PDM
Adjusted DM	652.40	3.93
PDM	3.93	1565.23

### *Error Due to Velocity*

Figures 3.11 and 3.12 show the dynamic DGPS error as a function of velocity for all survey nails. Data for both the direction of motion (raw and adjusted for latency) and perpendicular to the direction of motion is presented. In order to better inspect the latency adjusted error in the direction of motion, it was plotted separately in Figure 3.12. There is a slight trend of the data to more negative offsets with increasing velocities. This means that the GPS position data is lagging the actual vehicle position. This will have to be investigated further as more data at higher velocities is collected.

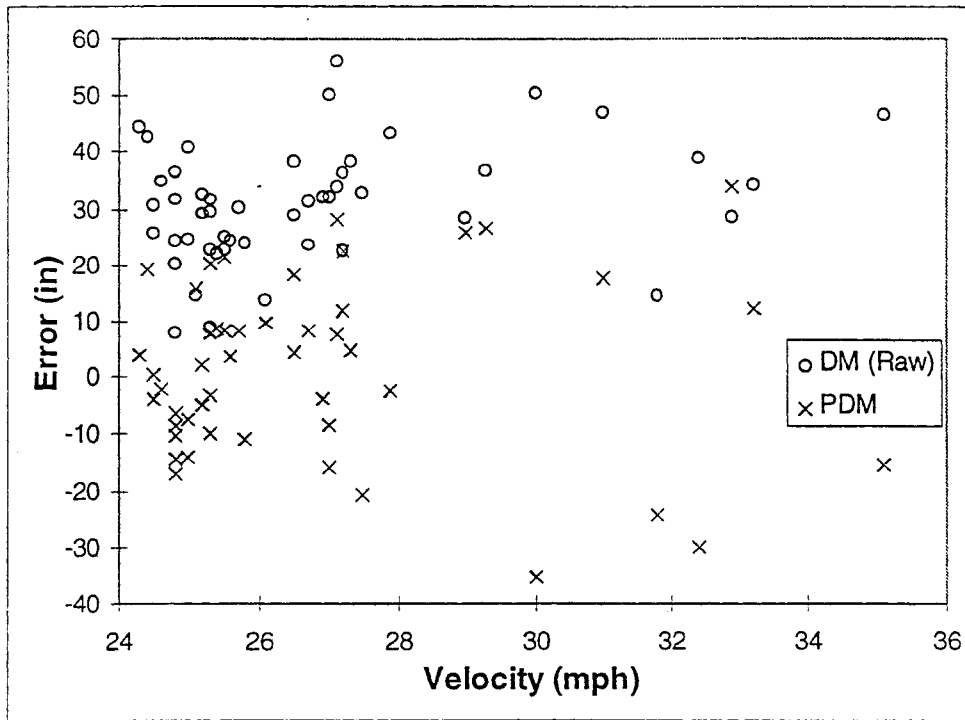


Figure 3.11 Raw DGPS dynamic error vs. velocity: 3/1/96 and 3/5/96 collected in the mid afternoon

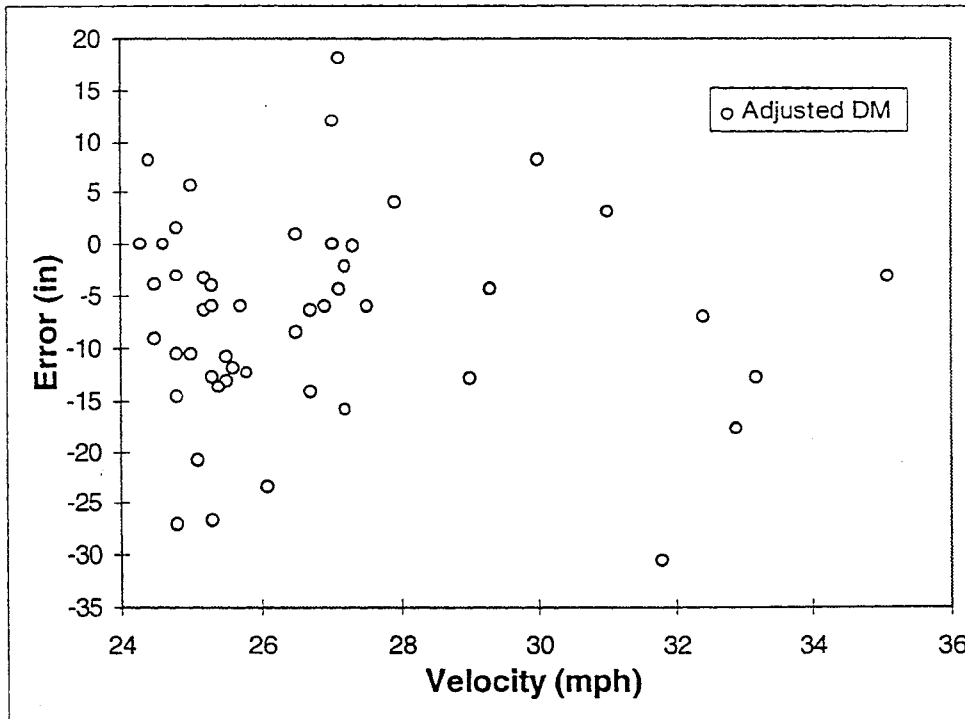


Figure 3.12 Latency adjusted DGPS dynamic error in the direction of motion vs. velocity: 3/1/96 and 3/5/96 collected in the mid afternoon

### *Dynamic DGPS Repeatability*

This study was done to better gauge the feasibility of generating a digital map with the DGPS system (see Section 2.2.2), and then to use such a map as a basis for tracking a vehicle, providing warning to the driver, and if necessary keeping the vehicle in the lane. This objective requires a reasonable degree of repeatability in the DGPS data while moving.

Figures 3.13, 3.14 and 3.15 show the raw DGPS position data taken while the truck drove 6 laps around the outside lane of the Mn/ROAD track. Figure 3.13 shows the path that the truck took based on the DGPS data (converted to state plane coordinates). This path matches almost exactly to the shape of the track (Figure 1.2). Figures 3.14 and 3.15 show magnified views of the laps. The width of the separation between the six laps ranged between 35.1 cm (1.15 ft) and 64.3 cm (2.1 ft). This range of variation compares favorably with the dynamic results described earlier. Note that a portion of this error is associated with the driver's limited ability to repeatably follow the exact same trajectory around the course. As such it is difficult to assign an exact dynamic repeatability to the GPS data itself.



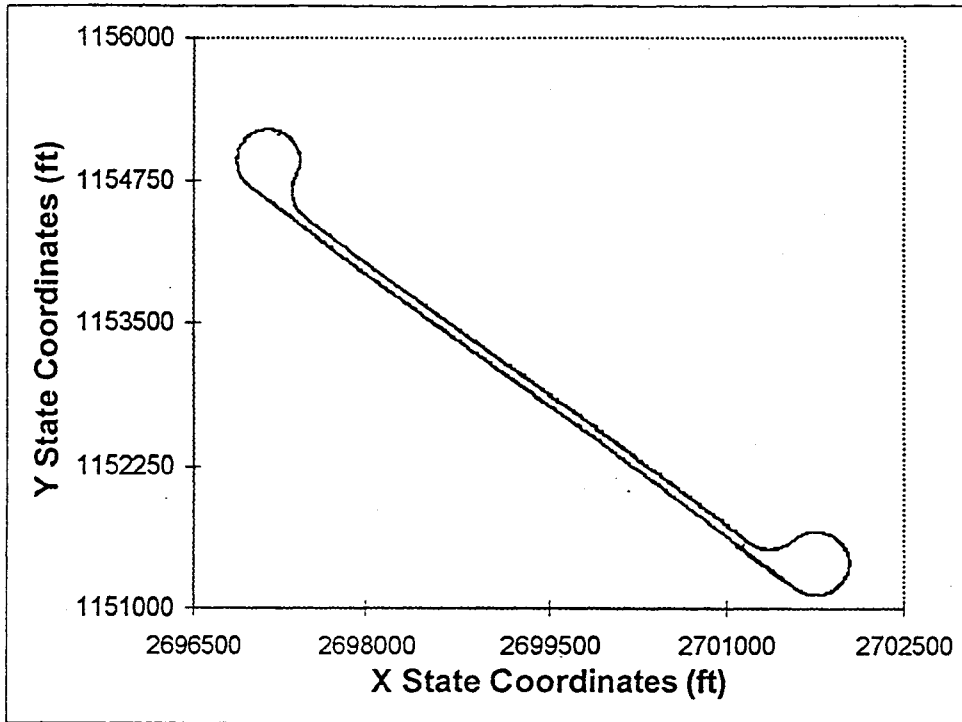


Figure 3.13 10/26/95 Dynamic test: DGPS logged during 6 laps at Mn/ROAD

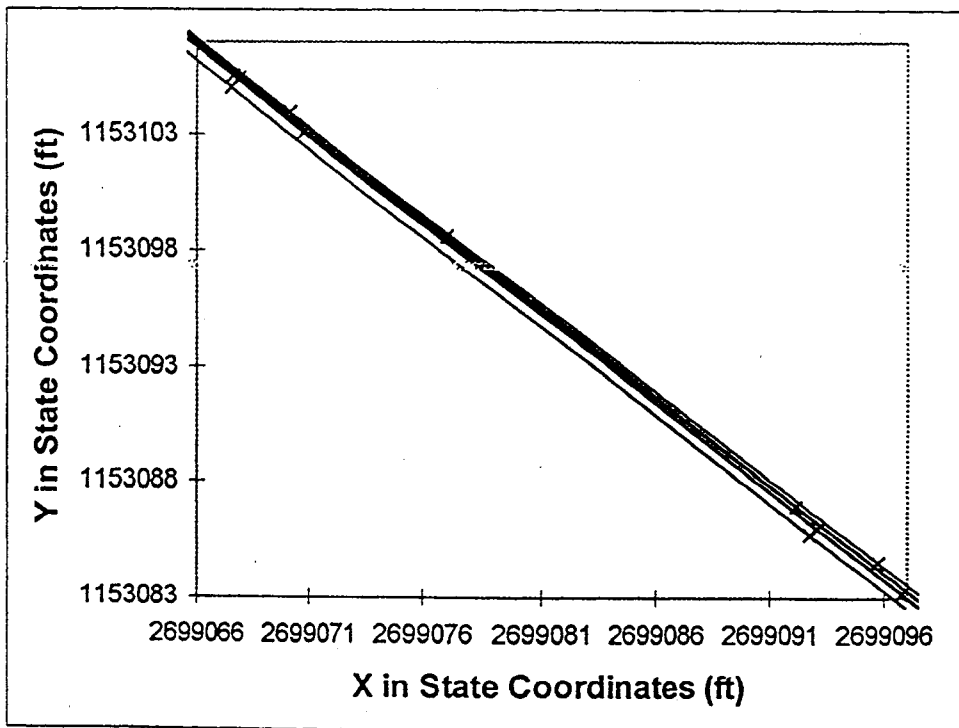


Figure 3.14 10/26/95 Close-up of straight section of 6 laps at Mn/ROAD. Tick mark indicates GPS data collected at that point.

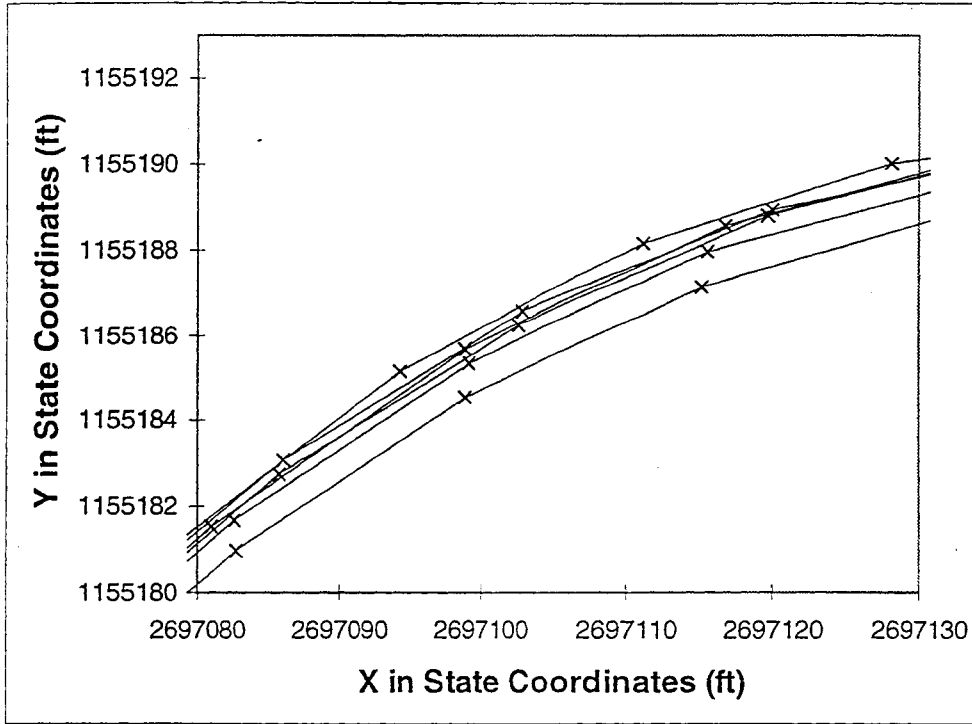


Figure 3.15 10/26/95 Close-up of northwestern curve section of 6 laps at Mn/ROAD

## CHAPTER 4

### Conclusions

The errors for the dynamic tests were considerably larger than for static results. Increased error is to be expected for the dynamic tests, given the nature of the DGPS system. Our goal was to evaluate whether the error using the newer DGPS technology is sufficiently small so as to allow us to detect a vehicle leaving its lane before it is too late to take corrective action. We believe that the results show that the DGPS in concert with other sensors will indeed provide us with the needed information. We showed that a significant portion of the GPS latency effects can be removed if the latency is characterized correctly. However, a small dependency of the DGPS accuracy on the longitudinal velocity of the vehicle was still present after removing the latency effect. The relatively small mean offsets after the latency adjustment indicate that there is residual deterministic error. Integrating the DGPS system with an inertial measurement unit should improve our ability to track the vehicle motion since this should reduce the effects of the GPS stochastic error. The results determined at this stage are being incorporated into the final implementation of the Kalman filter for estimating the states of the vehicle.

Errors that we did not account for must be considered in weighing our results. One such error is due to the camera tilting with the vehicle up to an angle of 10 degrees with respect to the vertical (vehicle roll axis) because of the road/shoulder incline. We expect that quantification of this type of error can lead to further improvement of the GPS data through the use of the roll rate gyro of the IMU. The gyros that we are using can sense angular rates as small as  $\pm 0.02$  deg/sec and as large as  $\pm 100$  deg/sec. The dynamic tests that we discussed here were conducted at speeds up to 35 mph. With an independent measurement of the instantaneous velocity vector and of the actual latency, we expect that we can significantly reduce the effect of latency. Tests at higher speeds are planned for the near future.

For many reasons, including safety and reliability concerns, no one sensor can provide all the information needed for the task that we propose, yet GPS does show potential for providing one significant component, especially given the many other applications for knowing the vehicle location. Repeatability is the important measure of the ultimate utility of the GPS in this application since measuring lane departure is achieved by comparing the real time lateral position measurement against a digital 'map' which stores the previously digitized lane trajectories. Achievable repeatability is almost always better than accuracy. Furthermore, in evaluating our results, keep in mind that the location uncertainty of the surveyed nails themselves ( $\pm 6$  cm in longitude and  $\pm 3$  cm in latitude).

Actual tests that we conducted indicated that the time required for reconvergence to the needed accuracy following a complete block of the receiver (as would be the case for going under an overpass) was much too long. However, our objective was to demonstrate the technology on the Mn/ROAD site, where no such obstructions are present. We also feel that newer GPS receivers now becoming available, such as those utilizing dual frequency receivers, which exhibit much shorter convergence times (on the order of 1 minute) may solve this problem.

Even though the cost of the systems described here are still high, further technology and manufacturing improvements will drive the cost down as the market demand leads to higher volume production. Furthermore, the demand for GPS provided position data for a myriad of other applications from aircraft control during landing to tracking commercial vehicles will lead to the proliferation of more differential base stations transmitting correction data.

In the next phase of our work, we plan to incorporate a suite of other sensors and analytical tools to more accurately measure and confirm our results. In the future, we expect to compare the instantaneous vehicle velocities as determined from the images to that derived by integrating a lateral and a longitudinal accelerometer on the vehicle. We plan to compare the vehicle yaw angles with respect to north as determined from the images to those derived by integrating a yaw rate gyro on the vehicle. We are in the midst of improving the accuracy of the image processing by using automated imaging algorithms which can take measurements at subpixel accuracy. We will then use a roll gyro to compensate for the vehicle roll's effect on the camera position. Experiments that more directly measure the latencies in the GPS system are under way. We plan to run more long-term tests of the DGPS system to better understand the 12 hour oscillatory behavior, its contributing factors and its effect on the system accuracy. We hope to be able to compensate for this behavior, thus improving the accuracy of the overall system.

All of these results will allow us to more reliably use the data for monitoring a truck's motion in its lane and triggering appropriate action if the vehicle exhibits erratic behavior as would be the case if the driver were falling asleep at the wheel (or driving while intoxicated or under the influence of other substances).

## REFERENCES

1. Knipling, R. and Wang, J.-S., "Crashes and Fatalities Related to Driver Drowsiness/Fatigue," Research Note, NHTSA, November, 1994.
2. Shankwitz, C., Donath, M., Morellas, V. and Johnson, D., "Sensing and Control to Enhance the Safety of Heavy Vehicles," Proceedings of the Second World Congress on Intelligent Transport Systems, Volume 3, pp. 1051-1056 Yokohama, Japan, ITS America, November 1995.
3. Jacobs, G., Hopstock, D., Newell, R., Dahlin, T., Keech, R., Gonzales, B., Stauffer, D., Lenz, J., "A Magnetic Pavement Marking and Sensor System for Lateral Control/Guidance of Vehicles," Proceedings of the Second World Congress on Intelligent Transport Systems, Volume 3, pp. 1236-1241, Yokohama, Japan, ITS America, November 1995.
4. Pomerleau, D., Jochem, T., "Rapidly Adapting Machine Vision for Automated Vehicle Steering," *IEEE Expert*, pp. 19-27, April 1996
5. Galijan, R.C., Gilkey, J.Y, and Turner, R.P. "Carrier Phase GPS for AHS Vehicle Control," *U.S. Department of Transportation, Federal Highway Administration, Publication # FHWA-RD-96-052*, 1996.
6. Da, R. and Dedes, G., "Nonlinear Smoothing of Dead Reckoning Data With GPS Measurements," Proceedings of 1995 Mobile Mapping Symposium, The Ohio State University, pp. 173-182, May 1995.
7. He, G., "Integration of GPS and INS for a Mobile Mapping System," Proceedings of 1995 Mobile Mapping Symposium, The Ohio State University, pp. 85, May 1995.
8. Lipp, W., Sagrestani, V. and Sarrica, R. "Integrated GPS/Fibre Optic Gyro Land Navigation System," *Proceedings of the IEEE Position Location and Navigation Symposium*, pp. 447-452, 1994.
9. Mattos, P.G. "Integrated GPS and Dead Reckoning for Low-Cost Vehicle Navigation and Tracking," *Proceedings of the IEEE-IEE Vehicle Navigation and Information Systems Conference*, pp. 559-574, 1994.
10. Kobayashi, K. Watanabe, K and Munekata, F. "Accurate Navigation via Sensor Fusion of Differential GPS and Rate-Gyro," *Proceedings of the IEEE Instrumentation and Measurement Technologies Conf.*, pp. 556-559, 1994.
11. Leenhouts, P.P., "On the Computation of Bi-Normal Radial Error," *Navigation: Journal of the Institute of Navigation*, pp. 16-28, Vol. 32, No. 1, Spring 1985

12. Sreenivasan, S.V., and Waldron, K.J. "A Drift-Free Navigation System for a Mobile Robot Operatin on Unstructured Terrain," *Transactions of the ASME*, Vol 116, pp. 894-900, 1994.
13. Leick, A. *GPS Satellïte Surveying*. Wiley, 1995.
14. Lachapelle, G, Townsend, B., Gehue, H. and Cannon, M.E. "GPS versus Loran-C for Vehicular Navigation in Urban and Mountainous Areas," *Proceedings of the IEEE-IEE Vehicle Navigation and Information Systems Conference*, pp. 456-459, 1993.
15. Byrne, R.H., Karer, P.R., and Pletta, J.B. "Techniques for Autonomous Navigation," *Sandia National Laboratories Special Publication*, 1991.
16. Noe, P. and Zabaneh, K. "Relative GPS," *Proceedings of the IEEE Position Location and Navigation Symposium*, pp. 586-590, 1994.
17. Bullock, J.B. and Krakiwsky, E.J. "Analysis of the Use of Digital Road Maps in Vehicle Navigation," *IEEE Position Location and Navigation Symposium*, pp. 494-501, 1994.
18. Whitehorn, K.L. "The Minnesota County Coordinate System: A Handbook for Users," *Minnesota Assoc. of County Surveyors Special Publication*, 1995.
19. *Conad 83 Users Manual* 1995.
20. Johnson, G.W. "A Minnesota County Coordinate System," *Proceedings of the 33rd Annual Meeting of the Minnesota Land Surveyors Association*, 1985.
21. *JVC BR-S822DXU Video Cassette Recorder Operator's Manual*, JVC, 1994.
22. *Novatel GPSCard Command Descriptions Manual, revision 2.0*, 1995.
23. Denaro, R., "Navstar: The All-purpose Satellite," *IEEE Spectrum*, May, 1981.
24. Stem, J.E., "State Plane Coordinate System of 1983," NOAA Manual NOS NGS 5, National Geodetic Survey, Rockville, MD, 1989. .
25. Ford, T.J. and Neumann, J., "NovAtel's RT20 - A Real Time Floating Ambiguity Positioning System," *Proceedings of the 1994 ION GPS Conference, 7th International Technical Meeting of the Satellite Division of the Institute of Navigation, Salt Lake City, UT*, pp. 1067-1076, September 20-23, 1994
26. State of MN GPS Base Station Task Force Report, September 1994.

## Appendix A

### Coordinate Conversion Program

This program was written to convert the GPS position readings from global longitude/latitude to state plane coordinates. The exact conversion was calculated using the equations below. The equations and terms presented here are developed in [24]. I would like to acknowledge the generous help of Chen Fu Liao in the writing of this program.

The Conad 83 program [19] was used to convert the GPS reading in state plane coordinates into county coordinates (Wright County) to be able to compare the readings to the survey nails. The county coordinate system is developed in [18] and [20].

#### Conversion Equations for GPS Positions

$\Phi$ =Degrees Latitude

$\lambda$ =Degrees Longitude

N=north

E=east

a=6378137

b=6356752.3141403

$\Phi_0 = B_0 = 44.5014884140$

K=11914387.7514

$\lambda_0 = L_0 = 94.00$

$R_b = 6667126.8494$

$N_b = 100000$

$E_0 = 800000$

$$f = \frac{(a - b)}{a}$$

$$e = \sqrt{2f - f^2}$$

$$Q = \frac{\left[ \ln\left(\frac{1 + \sin(\Phi)}{1 - \sin(\Phi)}\right) - e * \ln\left(\frac{1 + e * \sin(\Phi)}{1 - e * \sin(\Phi)}\right) \right]}{2}$$

$$R = \frac{K}{\exp(Q * \sin(\Phi_0))}$$

$$\gamma = (\lambda_0 - \lambda) * \sin(\Phi_0)$$

$$Y = N = R_b + N_b - R * \cos(\gamma)$$

$$X = E = E_0 + R * \sin(\gamma)$$

/\*\*\*\*\*\*

convert.c - convert lat,lon into x,y coordinates  
Written by Chen Fu Liao and Robert Bodor

This program was written to convert the GPS position readings from global longitude/latitude to state plane coordinates. It reads the latitude and longitude coordinates from the GPS log and converts them to X and Y coordinates in the state plane coordinate system.

\*\*\*\*\*/

```
#include <stdio.h>      /* general I/O */
#include <string.h>
#include <math.h>       /* float math */
#include <dos.h>        /* time function */
#include <conio.h>      /* outp function */
#include "convert.h"
#define DataSize 255   /* 255 */
```

```
void main()
{
    unsigned char novatelData[DataSize]; /*GPS Log */
    char inchar ;
    unsigned char *lat, *lon, *sec ; /*Latitude, longitude, seconds */
    unsigned char *gdop, *pdop ;
```



```

double latVal, lonVal, gpsSec ;
double gdopVal, pdopVal ;
FILE *fpr, *fpw, *fp_gdop ;    /*Initializes file pointers */
int field ;
int i ;
double sin_phi0, sin_phi ;
double gama, Q, R, Ln1, Ln2 ; /*Initializes variables of */
double X, Y ;                  /* conversion equations */

sin_phi0 = sin(phi_0*deg2rad) ;
printf("\n\tHit \"ENTER\" to start ...");
do {
    inchar = getchar() ;
} while (inchar != '\n') ;

/* data conversion start here */
/* open a data file */
if ((fpr = fopen("c:/liao/mysource/gps_proj/gps5_3_1.dat", "r+")) ==
NULL)
    {   printf("\t *** Fail to open gps data file ***\n\r");
    }
if ((fpw = fopen("c:/liao/mysource/gps_proj/gps5_3_1.cnv", "a+"))
== NULL)
    {   printf("\t *** Fail to open P20 data file ***\n\r");
    }
/*

if ((fp_gdop = fopen("nov09/con101_3.dop", "a+t")) == NULL)
    {   printf("\t *** Fail to open GDOP data file ***\n\r");
    }
*/
while(fscanf(fpr,"%s\n", novatelData) != EOF)
{
/* printf("%s\n",novatelData);
*/
/*   printf("\tHit \"ENTER\" to start ...");
do {
        inchar = getchar() ;
    } while (inchar != '\n') ;
*/
if ((novatelData[1] == 'D') /* GDOP-A data */
    && (novatelData[2] == 'O')
    && (novatelData[3] == 'P')

```

```

        && (novatelData[4] == 'A'))
    {
        /* parse lon, lat data here */
        field = 0;
        for (i=0;i<DataSize;i++)
        {
/*      printf("novatelData[%d]=%c\n",i,novatelData[i]); */

            if (novatelData[i] == ',')
            {
                field++;
                switch (field)
                {
                    case 2: sec = &novatelData[i+1];break;
                    case 3: gdop = &novatelData[i+1];break;
                    case 4: pdop = &novatelData[i+1];break;
                }
            } /* if */
        } /* for */
        gpsSec = strg2val(sec);
        gdopVal = strg2val(gdop);
        pdopVal = strg2val(pdop);
        printf(" SEC = %-.2f sec\t",gpsSec);
        printf("GDOP = %-.4f\t",gdopVal);
        printf("PDOP = %-.4f\t\n",pdopVal);
        fprintf(fp_gdop, "%-.2f\t%-.4f\t%-.4f\n",gpsSec,gdopVal,pdopVal);
    }
    else if ((novatelData[1] == 'P') /* P20-A data */
        && (novatelData[2] == '2')
        && (novatelData[3] == '0')
        && (novatelData[4] == 'A'))
    {
/*      printf("novatelData=%s\n",novatelData);
        do {} while(getchar() != '\n');
*/

        /* parse lon, lat data here */
        field = 0;
        for (i=0;i<DataSize;i++)
        {
/*      printf("novatelData[%d]=%c\n",i,novatelData[i]);
        do {} while(getchar() != '\n');
*/

            if (novatelData[i] == ',')

```

```

        {
            field++;
            switch (field)
            {
                case 2: sec = &novatelData[i+1];break;
                case 5: lat = &novatelData[i+1];break;
                case 6: lon = &novatelData[i+1];break;
            }
        } /* if */
    } /* for */
/*for (j=0;j<12;j++)
{
    printf("%c",lat[j]);
}
*/

    gpsSec = strg2val(sec);
    latVal = strg2val(lat);
    lonVal = strg2val(lon);
    printf(" SEC = %-.2f sec\t",gpsSec);
    printf("LAT = %-.9f deg\t",latVal);
    printf("LON = %-.9f deg\t\n",lonVal);

    /* convert lon, lat into x, y here */
    gama = (lamda_0+lonVal)*sin_phi0*deg2rad;
/*
printf("\tgama = %f\n",gama); */
    sin_phi = sin(latVal*deg2rad);
    Ln1 = log((1.0+sin_phi)/(1.0-sin_phi));
    Ln2 = log((1.0+e*sin_phi)/(1.0-e*sin_phi));
    Q = 0.5*(Ln1-e*Ln2);
    R = K/exp(Q*sin_phi0);
    X = E0+R*sin(gama);
    Y = Rb+Nb-R*cos(gama);
/*
printf(" X = %-.6f M = %-.6f ft ",X,X*M2ft);
printf(" Y = %-.6f M = %-.6f ft\n",Y, Y*M2ft);
*/

    printf(" X = %-.6f M ",X);
    printf(" Y = %-.6f M\n",Y);
/*

    if ((fpw = fopen("pknail/8680_p20.dat", "a+t")) == NULL)
    {
        printf("\t *** Fail to open data file ***\n\r");
    }
*/

    fprintf(fpw,"%-.2f\t%-.6f\t%-.6f\n",gpsSec,X*M2ft, Y*M2ft);
} /* if-else if */
else
    continue;

```

```

    } /* while */
    printf("\n\tData conversion finished !!!\n");
    fclose(fp_gdop);
    fclose(fpw);
    fclose(fpr);
} /* main */

```

```

double strg2val(unsigned char *ptr)
{
    unsigned int index, READY;
    short sign, power;
    double value;
/* char inchar; */

    READY = 1;
    sign = 1;
    index = 0;
    power = 1;
    value = 0.0;
    if (*ptr == '-')
    {
        sign = -1;
        *ptr++;
    }
    do {
        if (*ptr == '.')
        {
            *ptr++;
            power = -1;
            index = -1;
        }
        if ((*ptr >= '0') && (*ptr <= '9') && (power > 0))
        {
            value = 10.0*value+(double)(*ptr-'0');
            *ptr++;
        }
        else if ((*ptr >= '0') && (*ptr <= '9') && (power < 0))
        {
            value = value+pow10(index--)*(double)(*ptr-'0');
            *ptr++;
        }
        else if (*ptr == ',')
        {
            READY = 0;
        }
        else
        {
            printf("\tError at \"strg2val\" function.\n");
            printf("%c\n", *ptr);
        }
    } while (READY);
/* printf("val=%f\n",value);
    do {

```

```
        inchar = getchar();
    } while (inchar != '\n');
*/
    } while (READY);
    return((double)sign*value);
}
```



## Appendix B

### Software Driver for Dynamic GPS Tests

This program interfaced with the DGPS system and the time stamp VCR and coordinated all of the data collection for the dynamic DGPS tests.

```
/******
```

Polling.c - Driver for Dynamic GPS Tests

Written by Robert Bodor with assistance from Chen Fu Liao and  
Sundeep Bajikar

This program initializes communication with both the GPS receiver and the VCR. It then commands the GPS to send a position log every 200 ms. Upon receipt of a GPS log, it queries the VCR for a frame number (time stamp) and records the time according to the computer clock. It then saves these 3 to file.

```
*****/
```

```
#include <stdlib.h>
#include <string.h>
#include <math.h>
#include <bios.h>
#include <dos.h>
#include <conio.h>
#include <stdio.h>
#define COM1 0
#define COM2 1
#define DATA_READY 0x100
#define TRUE 1
#define FALSE 0
#define SETVCR (_COM_9600 | _COM_CHR8 | _COM_STOP1 |
               _COM_NOPARITY)
#define SETGPS (_COM_9600 | _COM_CHR8 | _COM_STOP1 |
               _COM_NOPARITY)
#define play 0x3A
#define sense 0xDE
#define stop 0x3F
```

```

void main(void)
{

    int k,p,s,t;
    int i,j, count,time;
    unsigned in, outVCR[9], outGPS[206],out;

    unsigned status;
    unsigned val,val2,val3 ;
    char gpscmd[32],gpscmd2[32],gpscmd3[15],char1,char2 ;

    struct time sysTime, sysTime_new ;
    int cpu_hr, cpu_min, cpu_sec, cpu_hund ;
    int newcpu_hr, newcpu_min, newcpu_sec, newcpu_hund ;

    long sysTicks ;
    FILE *fp1;
    count=104;

    /* initialize the ports */
    _bios_serialcom(_COM_INIT, COM1, SETVCR);
    _bios_serialcom(_COM_INIT, COM2, SETGPS);

    /* open a data file */
    if ((fp1 = fopen("gps3.dat", "w+")) == NULL)
        {
            printf("\t *** Fail to open data file ***\n\r");
        }

    /* configure communication on GPS end */
    strcpy(gpscmd2,"COM2 9600 N 8 1 N off\n\r");
    for (i=0;i<23;i++)
    {
        val2 = gpscmd2[i] ;
        _bios_serialcom(_COM_SEND,COM2,val2);
    }

    strcpy(gpscmd,"log com2 P20A ONTIME 0.2 0.0\n\r");
    for (i=0;i<30;i++)
    {
        val = gpscmd[i] ;
        _bios_serialcom(_COM_SEND,COM2,val);
    }
}

```



```

printf("\n\n\t*** START DGPS DATA ACQUISITION ***\n");
/* read time from 486 CPU */
gettime(&sysTime);
cpu_hr = (int)sysTime.ti_hour;
cpu_min = (int)sysTime.ti_min;
cpu_sec = (int)sysTime.ti_sec;
cpu_hund = (int)sysTime.ti_hund;
/*
printf(" \t 486 CPU time =
%d:%d:%d.%d\n",cpu_hr,cpu_min,cpu_sec,cpu_hund);
*/

/* data acquisition start here */
for(;;)
{
/* read time from 486 CPU */
gettime(&sysTime_new);
newcpu_hr = (int)sysTime_new.ti_hour;
newcpu_min = (int)sysTime_new.ti_min;
newcpu_sec = (int)sysTime_new.ti_sec;
newcpu_hund = (int)sysTime_new.ti_hund;

/*main loop */

if (_bios_serialcom(_COM_RECEIVE,COM2,0) != NULL)
{

/* get VCR timestamp */

for(k=0;k<8;k++){
_bios_serialcom(_COM_SEND, COM1, sense);
outVCR[k] = _bios_serialcom(_COM_RECEIVE, COM1, 0);
putch(outVCR[k]);
}

/* get the GPS position data from Com 2 ... */

```

```

/* used to do it till: j<185 */
for(j=0;j<count;j++){
outGPS[j] = _bios_serialcom(_COM_RECEIVE,COM2,0);
putch(outGPS[j]);
}

/* write data to an output file */
fp1 = fopen("gps3.dat", "a");

fprintf(fp1,"\n
%d:%d:%d.%d\t",newcpu_hr,newcpu_min,newcpu_sec,newcpu_hund);

for(t=0;t<8;t++)
{
fprintf(fp1,"%c",outVCR[t]);
}
fprintf(fp1,"\n");

for (i=0;i<count;i++)
{
    fprintf(fp1,"%c", outGPS[i]);
}

fclose(fp1);

/* break and write to file if escape key is hit */
if (kbhit())
{
    if ((in = getch()) == '\x1B')
        break;
}

/* keep tracking the current data */
cpu_hr = newcpu_hr ;
cpu_min = newcpu_min ;
cpu_sec = newcpu_sec ;
cpu_hund = newcpu_hund ;
} /* if */
} /* main */

```

## Appendix C

### Offset Correction Program

This program is used to account for the offset distances between the pknail and the GPS antenna as the vehicle passes by the survey nail (as shown for example in Figure 37). It also checks the orthogonality of the tile to make sure the camera is exactly perpendicular to the ground.

The program takes in the digitized coordinates of the pknail, the center of the screen (GPS antenna), and the corners of the tile. The program then calculates the angle between the y axis in screen coordinates and north. Next, it calculates the distances in x and y (screen coordinates) between the pknail and the GPS antenna. It then converts the x,y distances into north and east, using the following conversion:

$$\begin{bmatrix} N \\ E \end{bmatrix} = \begin{bmatrix} \cos(\theta) & \sin(\theta) \\ -\sin(\theta) & \cos(\theta) \end{bmatrix} \begin{bmatrix} X \\ Y \end{bmatrix}$$

Once the offset distances between the GPS antenna and pknail are specified in north and east directions, they can be directly subtracted from the GPS position reading, thus accounting for the offset.

```
/*  
gpstest.c - converts coordinate frames
```

Written by Robert Bodor

This program takes in the four corners of the tile and the survey nail coordinates in screen coordinates from the data file (pa, pb, pc, pnail, pgps). It puts out the offset error in north and east directions (nerror and eerror), writing them to file.

```
*****/
```

```
/*gcc -lm gpstest3.c -o gpstest */  
#include <stdio.h>  
#include <math.h>  
#define NUMNAILS 60
```

```
double sqrt(double x);  
double sin(double x);  
double cos(double x);
```

```

double theta,angle,angle1,H,O,n1,e1,n2,e2,nerror,eerror,pi;
int pa[2],pb[2],pc[2],pnail[2],pgps[2],i,nailnum;

FILE *fpr,*fpw;int data[7];

main()
{
pi=3.14159265359;

/*
pa[0]=42;
pa[1]=136;
pb[0]=8;
pb[1]=76;
pc[0]=8;
pc[1]=136;
pnail[0]=42;
pnail[1]=136;
pgps[0]=159;
pgps[1]=121;
*/

fpr=fopen("nailcoords.dat","r+");
fpw=fopen("nailerr_12in_min90.dat","a+");

for(nailnum=0;nailnum<NUMNAILS;nailnum++){
fscanf(fpr,"%d %d %d %d %d
%d",&pa[0],&pa[1],&pb[0],&pb[1],&pnail[0],&pnail[1]);

pc[0]=pb[0];
pc[1]=pa[1];

printf("%d\t%d\t",pa[0],pa[1]);
printf("%d\t%d\t",pb[0],pb[1]);
printf("%d\t%d\t",pnail[0],pnail[1]);

H= sqrt((pa[0] - pb[0])*(pa[0] - pb[0]) + (pa[1] - pb[1])*(pa[1] - pb[1])) ;

/* O= (pa[0] - pc[0]); */
O=sqrt( (pa[0] - pc[0])*(pa[0] - pc[0]) + (pa[1]-pc[1])*(pa[1]-pc[1]) );

angle=asin(O/H)-90*pi/180;

```

```

printf("H= %f \n",H);
printf("O= %f \n",O);
printf("angle= %f \n",angle*180/pi);

/* This does the coordinate transformations */
n1=cos((pi/2)-angle)*pnail[0] + sin((pi/2)-angle)*pnail[1];
e1=cos((pi/2)-angle)*pnail[1] - sin((pi/2)-angle)*pnail[0];
n2=cos((pi/2)-angle)*pgps[0] + sin((pi/2)-angle)*pgps[1];
e2=cos((pi/2)-angle)*pgps[1] - sin((pi/2)-angle)*pgps[0];

/* This calculates the offsets in terms of north and east */
printf("n2= %f \n",n2);
printf("n1= %f \n",n1);
printf("e2= %f \n",e2);
printf("e1= %f \n",e1);
printf("n2-n1= %f \n",n2-n1);
printf("e2-e1= %f \n",e2-e1);

nerror=((n2-n1)*0.1677)*2.54;

error=((e2-e1)*0.1677)*2.54;

printf("nerror= %f cm\n",nerror);
printf("error= %f cm\n",error);

fprintf(fpw,"%d\t angle=%f nerror= %f cm\t error= %f
cm\n",nailnum+1,angle*180/pi,nerror,error);
}
fclose(fpr);
fclose(fpw);
}

```



## Appendix D

### Equations Used for Statistical Analyses

$$\text{Mean}(x) = E(x) = \frac{1}{n} \sum_{k=1}^n x_k$$

$$\text{Standard Deviation}(x) = \sigma(x) = \sqrt{\frac{n \sum_{k=1}^n x_k^2 - \left( \sum_{k=1}^n x_k \right)^2}{n(n-1)}}$$

$$\text{Covariance}(x, y) = E\{[x - E(x)][y - E(y)]^T\}$$

$$95\% \text{ Confidence Interval}(x) = \text{Mean}(x) \pm 1.96 \left( \frac{\sigma(x)}{\sqrt{n}} \right)$$

